Microtubule Affinity-Regulating Kinase 2 (MARK2) Induces the Early Morphological Changes Seen in Pathological Cardiac Hypertrophy

Michael Do

A thesis submitted in partial fulfillment of the requirements for the
Master's degree in Cellular and Molecular Medicine

Department of Cellular and Molecular Medicine
Faculty of Medicine
University of Ottawa

ABSTRACT

Cardiac hypertrophy, a compensatory growth response to various physiological and pathological stimuli, involves intricate cytoskeletal changes within cardiomyocytes. However, the molecular mechanisms governing these cytoskeletal processes is not yet well defined. Microtubule affinity-regulating kinase 2 (MARK2) is of particular interest as it plays an important role in controlling microtubule dynamics and cell polarity to define cell shape. In this thesis, we aim to determine whether MARK2 is involved in initiating the morphological alterations that drive cardiac hypertrophy. Our image analysis reveals a significant increase in total MARK2 signal during pathological remodeling, particularly in the initial hours. However, no significant change occurs under physiological hypertrophy. Inhibiting MARK2 significantly impacts cell area and length-to-width ratio during pathological remodeling but has no effect under physiological conditions. Additionally, MARK2 inhibition results in decreased microtubule density and reduced Tau phosphorylation at Serine262 in pathological remodeling cardiomyocytes. Furthermore, our findings indicate an increased number of binucleated cardiomyocytes in pathological hypertrophy, with MARK2 inhibition influencing this parameter. Overall, our findings provide clarity in the role that MARK2 has in driving cytoskeleton alterations to shift cell morphology in pathological cardiac hypertrophy and a unique potential therapeutic in preventing the transition to fulminant heart failure.

ACKNOWLEDGMENTS

First, I would like to thank my supervisor, Dr. Lynn Megeney, my TAC members, and all the past and current of Megeney's lab members. Second, I want to thank my parents Andrew Do and Halina Wladymiruk. I could not have done this without your love and support. Finally, I would like to thank my fiancée, Christa Henry, for your love, support, and patience with me as I made this journey and begin a new one (June 8th, 2024).

TABLE OF CONTENTS

List of Abbreviations

MARK2	Microtubule affinity-regulating kinase 2
PAR-1b	Polarity-regulating kinase partitioning-defective 1b
CDKs	Cyclin-dependent kinases
NVRMS	Neonatal rat ventricular cardiomyocytes
mTORC	Mechanistic target of rapamycin complex
mRNAs	microRNAs
ANP	Atrial natriuretic peptide
BNP	B-type natriuretic peptide
NRP1	ANP receptor 1
NFAT	Nuclear factor of activated T
GATA4	Gata binding protein 4
MEF2A	Myocyte-specific enhancer factor 2 A
MAPK	Mitogen-activated protein kinase
ERK1/ERK2	Extracellular signal-regulated kinases 1 and 2
JNK	C-Jun N-terminal kinases
p38	P38 mitogen-activated kinases
ET-1	Endothelin 1
IGF-1	Insulin-like growth factor 1
VEGF	Vascular endothelial growth factor
HIF1α	Hypoxia-inducible factor 1α
PI3K	Phosphatidylinositol 3-kinase

PIP	Phosphatidylinositol 4,5-bisphosphate
AKT	Protein kinase B
PDK1	Pyruvate dehydrogenase kinase 1
FAK	Focal adhesion kinase
Rho	Ras homolog family member
PKC	Protein kinase C
MEK5	Mitogen-activated protein kinase kinase 5
MTOCs	Microtubule organizing centers
PTMs	Posttranslational modifications
MAPs	Microtubule associated proteins
CAMKII	Calcium–calmodulin -dependent protein kinase II
Tau	Tubulin associated unit
HDAC	Histone deacetylase
aPKC	Atypical protein kinase C
GEF-H1	Guanine nucleotide exchange factor H1
PKD	Protein kinase D
ABP	Apical-basal polarity
PCP	Planar cell polarity
Scrib	Scribble planar cell polarity protein
JMEM	Joklik’s-modified Eagle medium
DMEM	Dulbecco’s modified eagle medium
SF	Serum-free
DMSO	Dimethylsulfoxide

PBS	Phosphate-buffered saline
DAPI	4’,6-diamidino-2-phenylindole
siRNA	Small interfering RNA
CTCF	Corrected total cell fluorescence
SEM	Standard error of the mean
PE	Phenylephrine
CT1	Cardiotrophin 1
IF	Immunofluorescence
pTauS262	phosphorylation of Tau at Serine262

List of Figures

CHAPTER 1: INTRODUCTION

THE DEVELOPMENT OF THE HEART

The fundamental function of the heart is to pump blood throughout the body, to deliver oxygen and nutrients to organs and to transport carbon dioxide back to the lungs. The heart can perform complex remodelling of its structure, growth, or retraction, as a response to various extrinsic and intrinsic stimuli [1]. These external demands, whether from normal growth or stress conditions, are necessary to maintain cardiac output and blood supply to the organism as a whole. This phenotypic plasticity of the heart is primarily characterized by changes in myocardial structure; specifically, the ventricular wall chamber may thicken to adjust the contractile output to maintain cardiac homeostasis [1,2]. For example, the left ventricle pumps blood at higher pressures compared to the rest of the other heart chambers, as it faces a much higher workload and mechanical afterload. As a result, the free wall of the left ventricular wall is much thicker and has a greater mass in comparison to that of the right ventricle, which only needs to pump deoxygenated blood to the lungs [3].

During the neonatal period, the expansion in the size of the heart involves dramatic and rapid physiological and structural changes [4]. Various biochemical adaptations occur during this transition to the postnatal life including release of catecholamines, renin-angiotensin, and vasopressin to strengthen myocardial contractility and increase heart rate [4,5]. This leads to sufficient elevation of cardiac output in order to meet the increased metabolic demands from a transition to the extrauterine environment. Thus, the neonatal myocardium is initially more dependent on heart rate to increase cardiac output, but shortly thereafter, the growth of the left ventricle matches the increased demand in systemic circulation. Conversely, the right ventricle remodels to being the thin-walled, crescent shaped chamber that supplies the lower pressure pulmonary circulation [6]. The transition from birth to early post-natal life is accompanied by an

approximate 30-fold increase in myocardial mass, such that by 3–6 months of age, the classical left ventricular dominant pattern of adulthood is established, with any further heart growth is matched to meet the escalating demands of the overall growth in the size of the organism [7].

1.1 THE TRANSITION FROM HYPERPLASIA TO CELL HYPERTROPHY

The dynamic shift in structural integrity of the myocardium is coordinated and managed by concurrent changes in the structure of the primary contractile unit of the heart, referred to as cardiomyocytes. Cardiomyocytes constitute approximately 25%–35% of total cardiac cell number [8,9]. The mammalian heart undergoes two distinct and high regulated modes of growth: cell proliferation known as hyperplasia and cell growth known as hypertrophy (Figure 1.1). During development, the embryonic heart grows by proliferation of multipotent cardiac progenitor cells, derived from the mesoderm, proepicardium, and neural crest, followed by the eventual terminal differentiation of these committed cardiomyocytes in late fetal and early peri-natal life [10,11]. However, the heart loses its proliferation capacity in most mammals early in life soon after birth with a transition from hyperplasia to hypertrophy [10]. Cardiomyocytes terminally differentiate soon after birth with many studies examining expression of known cell cycle regulators to validate the switch [12-14]. Many of the positive cell cycle regulators are downregulated in adult hearts such as cyclins, the cyclin-dependent kinases (CDKs), while many negative regulators are upregulated such as CDK inhibitors [15,18]. In addition, neonatal rat ventricular cardiomyocytes (NVRMS) undergo centrosome disassembly that coincides with lost proliferation capacity and terminal differentiation [16]. Interestingly, centrinone treatment of human induced pluripotent stem cells (iPSC) derived cardiomyocytes leads to an increase in cell surface area resulting in a hypertrophic growth morphology [16,17]. At the morphological level, this transition is distinguished by a notable rise in myofibril density, the emergence of fully developed intercalated discs, and the development

of binucleated cardiomyocytes, suggesting that the transition to maturity requires a concurrent reduction in cell division machinery [18].

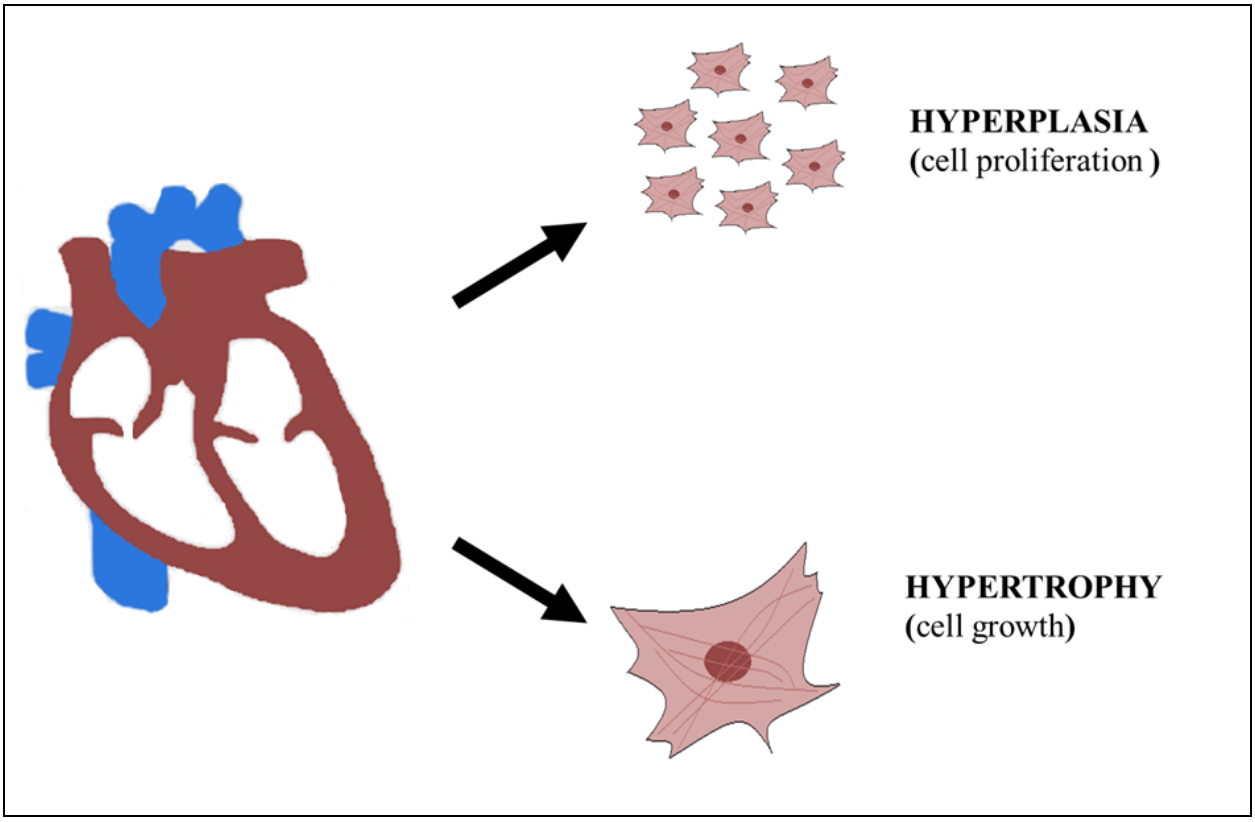

Figure 1.1. The Mammalian Heart and its Two Modes of Growth: Hyperplasia and Hypertrophy. During development, the embryonic heart grows by cell proliferation known as hyperplasia; however, the heart loses its proliferative capacity in most mammals early in life soon after birth with a transition from hyperplasia to cell growth known as hypertrophy.

More recently, the ability for adult cardiomyocytes to re-enter the cell cycle has been explored as a means to regenerate lost heart muscle mass, based on the prevailing assumption that myocytes retain a reserve capacity for DNA synthesis [19-21]. However, there is much debate and controversy surrounding the frequency and re-initiation of cell cycle mechanisms in post-natal cardiomyocytes. Key issues emerge including the accuracy of the assay used to monitor cell cycle activity and the capability to differentiate between cardiomyocyte nuclei and nonmyocyte nuclei [18]. Regardless, what is generally understood in the field is that any further growth of the heart muscle after birth is through hypertrophic development of the individual cardiomyocyte. With hypertrophic growth, cardiomyocytes undergo complete internal reorganization of cell structure to increase cell size, alter sarcomeric formation and increase production of protein synthesis, which translates into overall growth of the organ itself [2,6].

During the late fetal or early neonatal period, cardiomyocytes undergo one final nuclear mitosis and cell division resulting in a near doubling of the total number of single nucleated cells, 1 × 2N. In humans, DNA replication results in polyploidy of single nucleated cardiomyocytes, 1 × 4 + N, double nucleated, 2 × 2N cells representing only about 25% of all cardiomyocytes (Figure 1.2) [22-24]. The final ploidy step is somewhat different amongst mammals where mouse cardiomyocytes are primarily multinucleated whereas rabbits and rats exhibit predominantly binucleated hearts [22]. As a result, the total cardiomyocyte population of the heart is determined early in life and the number of viable myocytes dictates the cardiac function. In rodents, binucleation is a characteristic of terminally differentiated cells that are unable to proliferate, whereas mononucleate cells continue to cycle [12]. In humans, the fetal heart consists of mainly mononucleate cardiomyocytes and this is therefore the time at which most proliferation occurs. Just before birth, binucleation begins and can extend into early neonatal life [25]. Ploidy is positively related to heart weight and

increases further in response to injury [12,26]. The significance of polyploidization remains unclear, although it is proposed to be protective against hypoxia-induced apoptosis while being considered maladaptive for aerobic metabolism [27].

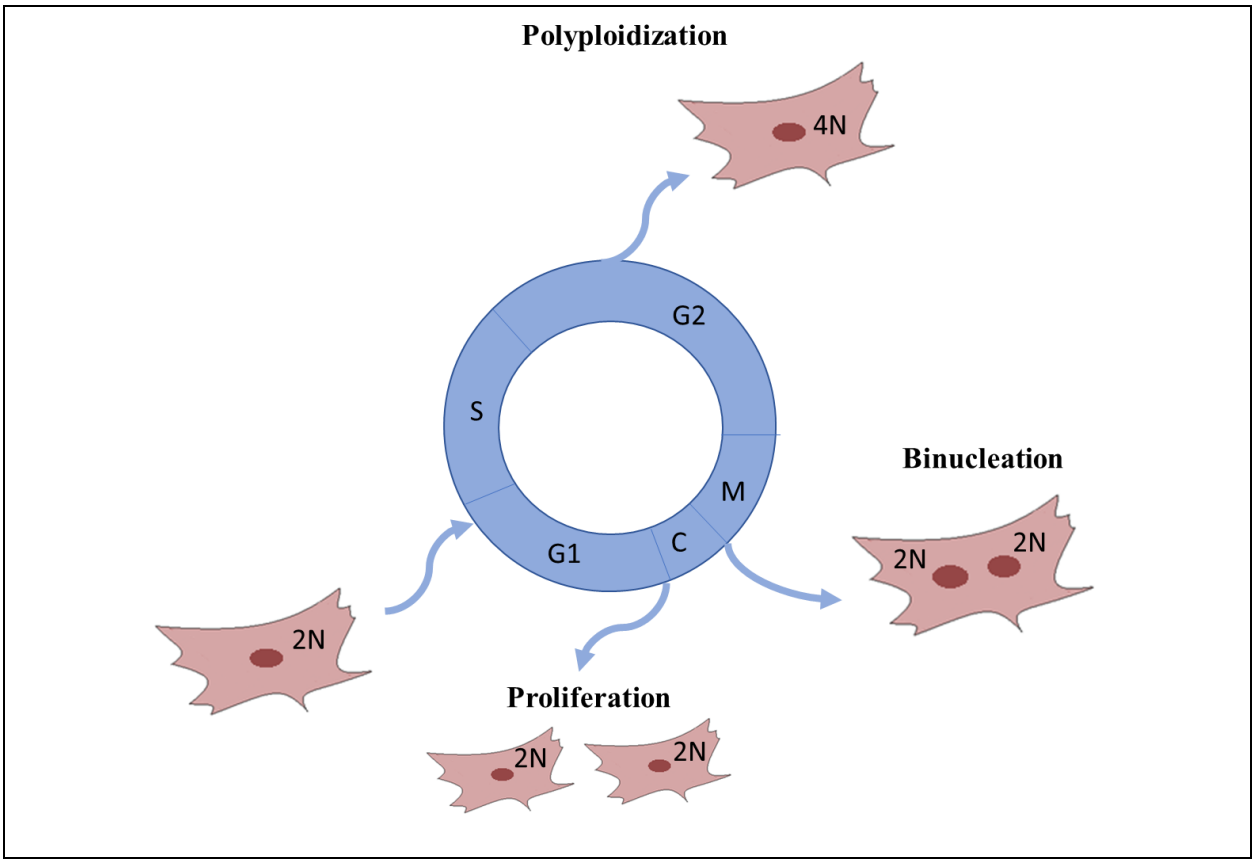

Figure 1.2. Cardiomyocyte Cell Cycle Activity. In the course of cardiomyocyte development, the heart undergoes growth primarily through the proliferation of cardiomyocytes. However, prior to birth, there is a decline in cardiomyocyte proliferation, and a substantial portion of neonatal cell-cycle activity is characterized by incomplete cell cycles. Cardiomyocytes opting for endoreplication exit the cell cycle post-S phase, transitioning into a polyploid state. Notably, karyokinesis without cytokinesis results in the binucleation of a majority of cardiomyocytes and the inability to proliferate.

1.2 MYOCARDIAL GROWTH IN ADULT HEARTS, THE MORPHOLOGY OF PHYSIOLOGICAL VS PATHOLOGICAL HYPERTROPHY

In an adult organism, at maturity, the heart can continue to undergo hypertrophic growth in response to increased demands and/or pathologic stimuli. Broadly, these forms of myocardial growth are referred to as physiologic and pathologic hypertrophy, reflecting either a beneficial or detrimental remodeling and expansion of the heart [28,29]. In humans, cardiac hypertrophy has been classified under two forms, physiological and pathological, and is dependent on the hypertrophic stimuli and the nature of the downstream signalling mechanism (Figure 1.3) [28-31]. Volume-overload stress, often stimulated by endurance exercise training, induces physiological hypertrophy growth leading to an increase in the internal diameter of the left ventricular as well as a proportional increase in the thickness of the ventricle wall [29,30]. Overall, physiological hypertrophy leads to enlargement of the ventricular chamber and an eccentric pattern of hypertrophy with increased ventricular stroke volume and cardiac flow at normal pressures. A form of physiological cardiac hypertrophy also occurs in the mother during the second and third trimesters of pregnancy, where cardiac output rises to match with the increased blood flow to the placenta, ensuring the necessary support for the developing fetus [32]. Similar to endurance exercise training, pregnancy results in sustained volume overload and the heart responds by undergoing modest eccentric cardiac hypertrophy, which is fully reversed in the months after delivery, when cardiac loads return to normal [32].

Alternatively, pressure-overload stress, causes concentric growth or pathologic hypertrophy, characterized by increased ventricular wall thickness and cardiac mass with little to no change in chamber volume [28,29]. Concentric cardiac hypertrophy may serve as a compensatory form of growth initially, to provide a mechanical advantage that helps normalize ejection

performance of the heart in the face of increased workload [33]. The classic example of this compensatory adaptation is the hypertrophy that occurs in response to lost heart muscle mass following a myocardial infarction. While initially adaptive, such a chronic overload results in a more advanced form of concentric hypertrophy with a small, thick-walled left ventricle [33]. Similarly, untreated hypertension acts to increase pressure overload, where hypertrophy occurs to maintain blood flow in the face of increased vascular resistance, and while initially adaptive can lead to predictable and rapid functional decompensation [34,35]. As such, the different patterns of hypertrophy and their associated changes in ventricular architecture reflect differences in the ratio of ventricular internal dimension to wall thickness.

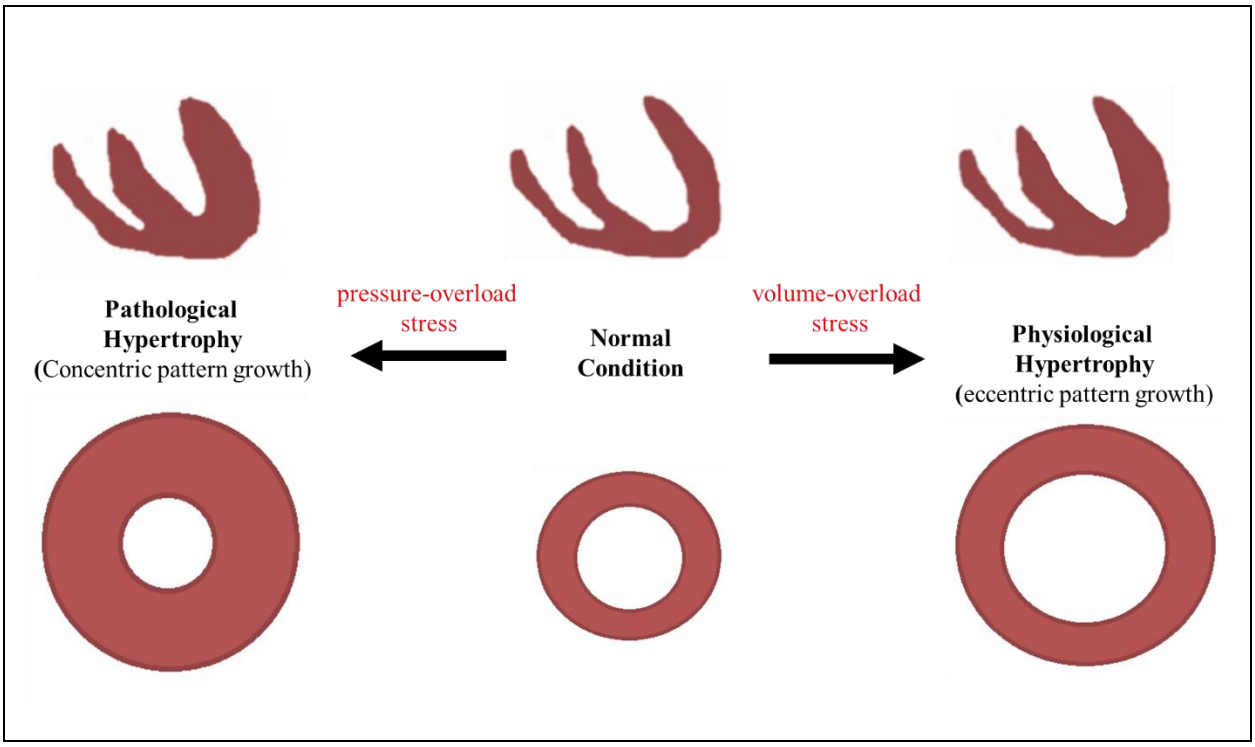

Figure 1.3. Concentric verses Eccentric Cardiac Growth on Ventricular Wall.

1.3 MOLECULAR PATHWAYS OF PATHOLOGICAL AND PHYSIOLOGICAL HYPERTROPHY

From a structural and functional aspect, pathological and physiological cardiac hypertrophy evolve from fundamentally different cellular architectures and associated signalling and transcription pathways. The development of pathological cardiac remodelling is accompanied by an intrinsic web of interconnected signalling pathways that lead to additional maladaptive outcomes [29]. These maladaptive outcomes may include: cell death, fibrosis, mitochondrial dysfunction, reactivation of fetal gene expression, impaired protein development, and mitochondrial quality control [29,36,37]. For example, a study has shown Ca2+/calmodulin-dependent protein kinase II, a conserved serine/threonine-specific induces the progression to maladaptive pathological remodelling of the heart by engaging ryanodine receptor 2-mediated Ca2+ leak from the sarcoplasmic reticulum resulting in a disruption of intracellular Ca2+ homeostasis in cardiomyocytes [38,39]. The mechanistic target of rapamycin complex (mTORC) pathway is another key player in the development of pathological cardiac hypertrophy. Activation of the mTORC1 pathway in response to various stressors, such as oxidative stress or pressure overload, has been shown to promote the growth of heart muscle cells, leading to an increase in heart size. Complete genetic disruption of mTORC1 or mTORC2 impairs the ability of the heart to respond to pressure overload and to undergo compensatory hypertrophy, resulting in the development of dilated cardiomyopathy [42]. Furthermore, many of the stress signalling pathways occur in the nucleus with the activation of a set of transcription factors, co-regulators, and microRNAs (mRNAs) [43]. Of these molecular changes occurring in pathological hypertrophy includes the reactivation of certain pathways observed during fetal cardiac development. These include an increase in the expression of genes encoding atrial natriuretic peptide (ANP) and B-type natriuretic peptide (BNP) as a

beneficial response to pathological stimuli. ANP and BNP can help to reduce the workload on the heart, improve blood flow, and reduce blood pressure [44-46]. Cardiac-specific deletion of the gene encoding ANP receptor 1 (NPR1) leads to mild hypertrophy that is exacerbated by pressure-overload stimulus, leading to pathological hypertrophy and cardiac remodelling [47].

The signalling pathways associated with pathological hypertrophy have been studied extensively and are far beyond the scope of this thesis. However, several pathways have been noted for their potent remodeling activity. For example, calcineurin is a Ca2+-activated serine-threonine protein phosphatase that dephosphorylates nuclear factor of activated T cells (NFAT) in the cytoplasm [48,49]. Activation of calcineurin/NFAT signaling is able to induce pathological cardiac by interacting with transcriptional cofactors, such as GATA Binding Protein 4(GATA4) or myocyte-specific enhancer factor 2 A (MEF2A), to stimulate expression of pathological hypertrophy-related genes [49]. Another well studied signaling pathway kinases involved in pathological hypertrophic growth includes the mitogen-activated protein kinase (MAPK) pathway. This large family of kinases includes the extracellular signal-regulated kinases (ERK1 and ERK2, often termed ERK1/2), c-Jun N-terminal kinases (JNK1, 2 and 3), p38 mitogen-activated kinases (p38α, β, γ and δ) or big MAP kinase (BMK or ERK5) [50]. The JNK and p38 branches of the MAPK cascade are collectively known as stress-activated MAPKs due to their specific responses to physical, chemical, and physiological stressors [51-54]. Both JNK and p38 are stimulated in cardiomyocytes by hormones that act on pathological heart growth, such as endothelin 1(ET-1), angiotensin II and phenylephrine [31], but only p38 is required for ANP expression and morphological changes observed during the development of myocyte hypertrophy [56]. Consistent with that observation, p38 activation mediates ET-1-induced GATA4 binding to BNP gene [57].

Unlike pathological cardiac hypertrophy, physiological hypertrophic remodelling occurs is fully adaptive accompanied by responses that are beneficial and reversable [34]. These responses include cell survival signalling, increased energy production and efficiency, angiogenesis proportional to the ventricular wall growth, and antioxidant systems [29,30]. For example, during the development of physiological hypertrophy, growth factors like insulin-like growth factor 1 (IGF-1) and vascular endothelial growth factor (VEGF) activate signalling pathways that promotes cell proliferation and survival [58]. Hypoxia-inducible factor 1α (HIF1α) is a major transcription factor that controls oxygen homeostasis by regulating angiogenesis, vascular remodelling, and glucose metabolism [59]. Physiological exercise training stimulates the production of HIF1α-responsive angiogenic factors, including VEGF. Additionally, the activation of the phosphatidylinositol 3-kinase (PI3K) signaling pathway is sufficient to increase myocardial fatty acid oxidative capacity and inhibition of PI3K signaling prevents mitochondrial adaptations in response to physiological hypertrophic [60]. Activated PI3K catalyzes the phosphorylation of phosphatidylinositol 4,5-bisphosphate (PIP2) to PIP3, which recruits protein kinase B (Akt) and Pyruvate Dehydrogenase Kinase 1 (PDK1) to the plasma membrane. Binding of Akt to PIP3 causes a conformational change in Akt, exposing the phosphorylation sites S473 and T308. Phosphorylation of S473 by mTORC2 and T308 by PDK1 activates Akt allowing for numerous downstream protective physiological changes to the heart (via Akt dependent and Akt independent mechanisms) [61].

The signalling and transcriptional associated with physiological and pathological cardiac hypertrophy help to further establish the difference between the two forms leading to increased cardiomyocyte size, protein synthesis, organelle alterations, and expression of genes [62]. Although numerous mechanisms of pathological and physiological cardiac hypertrophy have been well

documented, much is still required in understanding the early morphological and physiological changes.

1.4 CONTRIBUTION OF SARCOMERIC ARCHITECTURE TO HYPERTROPHIC GROWTH OF CARDIOMYOCYTES.

Observations from studies have shown that the organ level remodelling response starts with morphological changes within individual cardiomyocytes of the heart altered expression and modifications of sarcomeric and non-sarcomeric cytoskeletal regulators [63,64]. Although growth occurs in both cases, the molecular pathways underlying pathological and physiological cardiac hypertrophy significantly differ, leading to distinct structural and functional phenotypes (Figure 1.4) [65]. Many studies have examined in-detail the sarcomeric aspect of growth, establishing that under physiological cardiac hypertrophy, myocytes alter their morphology to favour cell growth by adding sarcomeres in series with a longer length-to-width ratio leading to an eccentric growth [1,33]. The addition of sarcomere in series within the growing cardiomyocytes increases cardiac output and volume load. In contrast, pathological hypertrophy is a form of concentric growth, characterized by adding sarcomeres in parallel, which leads to spatial growth and increased cell size but no change in the length-to-width ratio [1,33]. By adding sarcomeres in parallel to existing sarcomeric structures there is a modest increase in cardiac output. Interestingly, new sarcomeric formation has been noted in specific subdomains of the heart suggesting that pressure overload may be differentially translated across the myocardium [66].

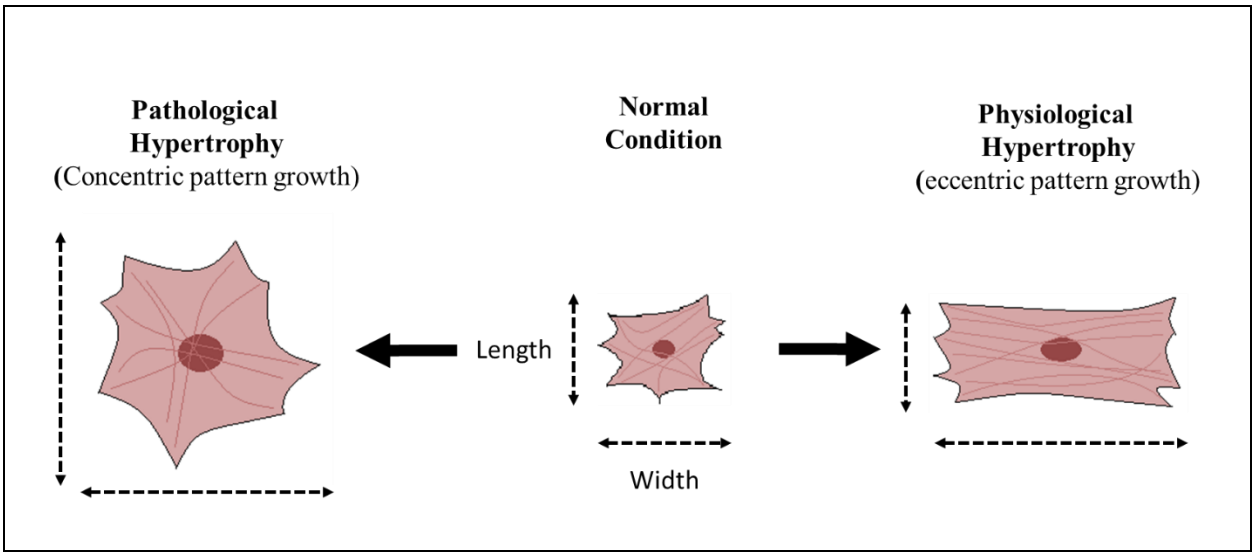

Figure 1.4. Pathological and Physiological Remodelling of Cardiomyocytes

The regulation of sarcomeric growth is directly responsive to mechanical stimuli, however, the molecular mechanisms surrounding the control of growth during new sarcomere addition in the adult myocyte remains poorly understood. Specifically, cardiomyocytes are almost crystalline in protein architecture, and it is difficult to understand how new elements might be added in a mature fiber under the constraint of continued force production generated by cyclic contractions. Clues to understanding the length remodeling processes may be provided by study of the general cell mechanosensory apparatus of the focal adhesion complex, which involves many proteins including: integrins, paxillin, focal adhesion kinase (FAK) and ras homolog family member (Rho) [67]. For example, observations by Ingber and colleagues suggest that mechanical deformation of integrins is the initial stage in an intracellular signaling cascade, triggering widespread cytoskeletal rearrangements and mechanotransduction at various remote sites within the cell [68]. Other studies suggest that the activation of the epsilon isoform of protein kinase C, PKCε, may play an important role in the process of recruiting and rearranging sarcomeric components [69-71]. Overexpression of active PKCε was sufficient to induce dramatic alterations in myocyte cell shape, leading to an overall increase in cell length, length-to-width ratio, and perimeter-to-area ratio [72,73]. These changes appeared similar to the alterations in myocyte shape produced by leukemia inhibitory factor via a mitogen-activated protein kinase kinase 5 (MEK5) and ERK5 signaling pathway [72,74]. Furthermore, PKCε co-localizes with FAK in myocyte focal adhesions and costameres.

1.5 THE ROLE OF MICROTUBULE STRUCTURE IN CARDIOMYOCYTE HYPERTROPHY

In addition to an increased sarcomeric structure, hypertrophy of cardiomyocytes must be accompanied by a matching adaptation in the cytoskeleton, which is the ultimate arbiter of cell

size and shape. Indeed, proper positioning, regulation, and turnover of sarcomeric components are managed by microtubules and intermediate filaments [75-77]. Microtubules are stiff polymers of α- and β-tubulins, that form a higher order assembly containing 11–14 protofilaments that arrange into a hollow polymer with an outer diameter of roughly 25 nm. Microtubules are critical in many basic cellular functions, including cell division, migration, and transport of mRNA, proteins, and organelles [75]. They are nucleated from microtubule organizing centers (MTOCs) that contain γ-tubulin, which serves as a structural template for high efficiency nucleation. In mitotic cells, centrosomal MTOCs continuously play a role in nucleating microtubules for the cell's entire lifetime; however, when cardiomyocytes transform to post-mitotic cells shortly after birth, they undergo a disassembly of centrosome integrity [78]. Adult cardiomyocytes depend exclusively on non-centrosomal MTOCs located on the nuclear envelope, as well as associated Golgi and Golgi outposts, for nucleation [79].

In adult cardiomyocytes, microtubules function as units resistant to compression, providing balance or countering contractile tension within the context of the remaining cytoskeletal framework [80]. In addition, a portion of the microtubule population may be stabilized to help promote directional cell migration or polarized cell growth [81,82]. Although an appropriate population of microtubules is essential to maintain cell shape and intracellular transport functions, an overabundance of microtubules can interfere with the contractile function of cardiomyocytes by imposing a viscous load on the shortening sarcomeres during contraction, with normal contractile function being restored when the microtubules are depolymerized [76,77]. For example, delivery of colchicine, a microtubule-depolymerizing agent, to aortic-banded mice reduced hypertrophy and improved cardiac function compared with saline-treated controls [83]. It has also been suggested that rapid intense growth results in the dense layering of microtubules hindering

contractility, while slow gradual stimulus of hypertrophic growth leads to a lower increased density of microtubules [77,84]. However, the exact molecular mechanisms governing these changes is not yet well defined. Studies consistently show that microtubules play a larger mechanical role in pathologically remodeled than in healthy myocardium [85-87]. Proteomic assessments of human left ventricular tissue demonstrate a marked upregulation of intermediate filaments and tubulin isoforms in advanced ischemic, hypertrophic, and dilated cardiomyopathy [88]. In advanced heart failure, this proliferation of the non-sarcomeric cytoskeleton coincides with a loss in force-generating myofilaments, through an increased viscoelastic resistance concurrent with reduced force production [89].

1.6 POST-TRANSLATION MODIFICATIONS OF MICROTUBULE PROTEINS AND THE IMPACT ON CARDIOMYOCYTE HYPERTROPHY

A growing body of evidence supports the hypothesis that posttranslational modifications (PTMs) of tubulin alters cytoskeletal dynamics to favor microtubule network stabilization, which in turn impacts cardiac hypertrophy and heart failure [88,90-92]. For example, the most well studied PTM of the microtubule network in the heart is detyrosination, where the most C-terminal tyrosine of α-tubulin is removed [91,92]. The buckling, load-bearing behavior of microtubules is promoted by detyrosination, and detyrosination directly increases myocyte viscoelastic stiffness contributing to contractile dysfunction in cardiomyocytes from patients with heart failure [91,92]. Another PTM of interest is acetylation, catalyzed by the enzyme α-tubulin acetyltransferase 1 within the microtubule lumen [93]. Acetylation occurs on stable microtubules, but as a result, it enhances the microtubule's lifespan by increasing flexibility and its ability to resist damage [94]. Understanding these post-translational modifications is advancing due to the development of new biochemical techniques that enable the purification of modified tubulins or the detection of endogenous PTMs

[95-97]. However, the majority of these modifications still lack comprehensive study within the context of the heart.

Structural microtubule associated proteins (MAPs) can also influence the stability of microtubules either by blocking or recruiting severing proteins or by affecting the association of microtubules with other cytoskeletal elements including the sarcomeres. Within MAPs, MAP4 has been widely studied to show that its expression is significantly increased in heart disease leading to an increase tubulin expression and microtubule stability [98-101]. This excessive MAP4 decoration of microtubules increases network density and stability, which can inhibit and jam motor-based transportation preventing cargo delivery in affected cells [102]. Additionally, phosphorylation of MAPs is a common regulator of MAP-microtubule affinity, which can have a pronounced effect on microtubule dynamics and network architecture**.** Interestingly, dephosphorylation of MAP4, which is demonstrated in pressure-overload hypertrophy, increases its association with and stabilization of cardiomyocyte microtubules [98,100]. By contrast, phosphorylation of MAP4 reduces its microtubule affinity and can destabilize the network, which may also lead to pathological remodeling [103]. As a result, a proper balance of de- and re-phosphorylated MAP4 (and by extension hyper- and hypo-stabilized microtubules) is optimal for the heart, and shifting of the equilibrium in either direction can lead to pathological remodeling. These examples demonstrate a robust ability to fine tune cardiomyocyte adaptation through combinatorial use of PTM and MAPS manipulation of the microtubule network.

Additionally, a canonical role of microtubules is the transport of cargo throughout the cell and in cardiomyocytes this transport function is essential for membrane remodeling and ion channel trafficking, with a common end point being an increased protein translation linked to growth of the cell. Recent work demonstrates an essential role for microtubules in spatially

coupling increased protein translation to productive growth of the heart through microtubule-based transport of mRNA and ribosomes [104]. Interestingly, subcellular localization of mRNA appears to be a potential candidate for how cardiomyocytes might initiate sites of new sarcomere addition. For example, in chick embryo fibroblasts, β-actin mRNA exhibits prominent localization at the leading edge, leading to heightened actin synthesis crucial for cell motility. Consequently, the disturbance of β-actin localization proves adequate to diminish cell motility, establishing a potential link between mRNA localization and adaptive morphological changes [105]. In aligned neonatal cardiomyocytes, the intracellular movement of α-cardiac actin mRNA ceases following a hypertrophic stimulus, and this redistribution is contingent upon microtubules [104].

1.7 MICROTUBULE AFFINITY-REGULATING KINASES. DO THESE REGULATORY PROTEINS INFLUENCE CARDIOMYOCYTE HYPERTROPHY?

Alterations in microtubule structure and function exert a notable influence on cardiomyocyte hypertrophy, yet the protein regulatory networks that govern microtubule dynamics remain poorly understood. One group of proteins that may exert control over microtubule dynamics during cardiomyocyte cell growth are the microtubule affinity-regulating kinases. MARKs are structurally similar to the serine/threonine-specific kinase calcium–calmodulin -dependent protein kinase II (CAMKII), which itself has been shown to act as a potent inductive cue for pathologic hypertrophy [106-109]. For example, a recent study has shown that a MARK family kinase, MARK4, phosphorylates MAP4 which in turn targets a microtubule detyrosinating protein vasohibin2 to reduce cardiomyocyte contractility in the ischaemic heart [110]. In addition to MARK4, MARK2 appears to be an impactful member of this kinase family, working a similar function as well as a role in maintaining cell polarity structure of the cell [111]. MARK2 is also known as polarity-regulating kinase partitioning-defective 1b (Par1b) and as the name suggests this kinase has been

shown to establish cell polarity [112-115]. Previous research has shown that MARK2 contributes to structural abnormalities and degeneration of neurons in Alzheimer's disease, which has similar genetic and proteomic profiles to heart failure [116-119]. In addition, MARK2 has been shown to regulate tubulin associated unit (tau) protein, which is important for microtubule stability, and whose deficiency results in impaired cardiovascular performance in mice [120]. Interestingly, MARK2 has been directly associated with many molecular pathways that stimulate pathological cardiac hypertrophy including mTORC pathways and class II histone deacetylase-based transcription mechanisms (HDAC)4/5 [121,122]. However, the role of MARK2 in the structural remodeling of cardiac cells under physiological or pathological conditions remains unknown.

1.8 MARK2, CELL POLARITY AND THE DEVELOPMENT OF CARDIOMYOCYTE HYPERTROPHY

MARK2 has been studied largely in the context of regulating cell polarity. Here, several studies have demonstrated that MARK2 controls asymmetric distribution of various cellular components and structures within a cell, critical for many cellular processes, including cell division, migration, and signaling [112-115]. MARK2 directly interacts with other proteins involved in regulating cell polarity such as with atypical protein kinase C (aPKC) complex, a group of enzymes that themselves promote cell polarity [112,113]. Furthermore, the interaction between MARK2 and aPKC has been shown to regulate the formation and maintenance of adherens junctions, structures that help to stabilize cell-cell contacts and maintain tissue architecture [123,124]. MARK2 activation can lead to the activation of various signaling pathways, including the indirect regulation of the Rho family via phosphorylation of guanine nucleotide exchange factor H1 (GEF-H1) to regulate RhoA [120]. Not only does RhoA regulate actin stress fibers, critical for the structural integrity of cardiomyocytes, but also the activation and translocation of mRNAs [125,126]. Lastly,

studies on Jurkat-Daudi cell conjugates revealed that the T cell receptor stimulation results in the phosphorylation of MARK2 by PKC and protein kinase D (PKD), resulting in its association with the 14-3-3 protein, followed by detachment from the cell membrane and accumulation at the promote MTOC reorientation [127].

Accordingly, these observations suggest that changes in the activity of core cell polarity regulatory proteins, such as MARK2, may influence the development of cardiomyocyte hypertrophy. This is not an unreasonable suggestion as the apical-basal polarity (ABP) and planar cell polarity (PCP) pathways have been shown to affect heart development [128,129]. For example, disruption in a number of key genes associated with polarity control, including protein kinase C iota and protein associated with LIN7 1, have been shown to result in marked abnormalities in the formation of the heart tube in the early zebrafish embryo [126]. More importantly, deletion of scribble planar cell polarity protein (Scrib) gene, involved in both ABP and PCP, disrupts cardiomyocyte organization and leads to abnormalities in the ventricular myocardium in mice [127,128]. Lastly, RhoA is involved in the regulation of the apical-basal polarity pathway and cytoskeletal formation. RhoA serves as a pivotal regulator in actin dynamics, playing a central role in the maintenance of cytoarchitecture, and as noted previously, has a complex role in inducing both cardioprotective signalling and pathologic hypertrophy [129,130].

1.9 RATIONALE

Our understanding of the role of PTMs and MAPs in cardiomyocyte growth and development continues to expand. However, what remains largely unknown is how signaling pathways and proteins manage the ultrastructural adaptations that are required for the pathologic growth of cardiomyocytes. The current understanding of MARK2 to establish cell polarity as well as maintain cytoskeletal networks [112,113,135,136], suggests that this kinase may act as a focal point in

controlling cell size adaptation. Additionally, previous research has shown that MARK2 contributes to structural abnormalities and degeneration of neurons in Alzheimer's disease, indicating that this kinase retains the capacity to induce cell structure pathology [116]. However, no current studies have been undertaken to determine the role MARK2 in the development of cardiac hypertrophy in cardiomyocytes. Therefore, the purpose of our study is to determine whether MARK2 is involved in initiating the morphological alterations that drive pathologic cardiomyocyte remodeling/hypertrophy.

1.10 HYPOTHESIS AND AIMS

We hypothesize that MARK2 regulates cardiomyocyte hypertrophy by inducing cytoskeletal reorganization. We further hypothesize that MARK2 may have divergent roles in the induction of physiological versus pathological cardiomyocyte hypertrophy.

Aim 1: Investigate whether MARK2 expression is altered in NRVMS during cardiomyocyte hypertrophy.

Aim 2: Determine whether MARK2 has different effects during pathological and physiological cardiomyocyte hypertrophy.

Aim 3: Study the downstream effects of MARK2 in cardiac hypertrophy.

CHAPTER 2: METHODS AND MATERIALS

2.1 ANIMALS

All animal studies (primary cell retrieval) were approved by the University of Ottawa Animal Care Committee. Sprague-Dawley rats were obtained from Charles River Laboratories (Wilmington, MA, USA). ACVS Protocol: OHRIe-3970 [Replacing OHRI-3734]-A1; Titled: Effects of Cardiotrophin-1 on rat primary cardiomyocytes; Principal Investigator: Dr. Lynn Megeney lmegeney@ohri.ca 737-8618

2.2 NEONATAL RAT PRIMARY CARDIOMYOCYTES

Primary neonatal rat cardiomyocytes were freshly isolated from hearts of 2-day-old Sprague-Dawley rats (Charles River Laboratories). Hearts were excised and placed in Joklik's-modified Eagle medium (JMEM). Ventricles were separated from the atria, minced with scalpel blades, and transferred to a 50 ml Falcon tube for digestion with 200 units per ml of Collagenase II (Worthington) in a total of 10 ml JMEM at 37 °C with gentle agitation. After 15 min, use a 25 ml pipet was used to slowly triturate (pipet up and down) the tissue and media 2-3 times and then briefly wait for the tissue to settle at the bottom of the pipet. Then, the tissue slurry was pipetted into a clean tube for further Collagenase digestions while discarding the remaining supernatant ("Digestion #0"), which contained cell debris.

Following this first digestion step, another 4-5 rounds of Collagenase digests were performed on the minced/digested heart tissue (as above); however, the supernatant (containing an appreciable number of primary cardiomyocytes) in these latter steps was transferred to a tube containing 10 ml of fetal bovine serum to stop the Collagenase reaction. This tube was centrifuged at 100× g for 5 min at room temperature to pellet the intact cells. The supernatant was discarded, and the cells were resuspended in 1 ml Dulbecco's Modified Eagle Medium (DMEM) growth

medium and each 1 ml cardiomyocyte fraction from the Collagenase digests were then pooled into one tube. The volume of pooled cardiomyocytes was then transferred onto a 70 µm filter pore size cell strainer (CellTreat) assembled on top of a 50 ml Falcon tube to help further remove cell clumps and cell debris. The cell strainer was then washed with an additional 25ml of DMEM growth medium.

Next, a pre-plating step was performed (to separate out cardiac fibroblasts and enrich for cardiomyocytes) by transferring the entire volume of flow-through onto a sterile 15 cm tissue culture dish, which was incubated at 37 °C for 30 min. Fibroblasts adhere to the dish while cardiomyocytes remain in the media. The media was then carefully collected using a 25 ml pipet and transferred to a new sterile 15 cm tissue culture dish for another round of pre-plating to further enrich for cardiomyocytes. After the second pre-plating incubation, media was transferred to a sterile tube and centrifuged at 100× g for 5 min at room temperature. The supernatant was then discarded and resuspended in 5 ml of DMEM growth medium to yield the primary cardiomyocyte cell stock.

The number of cardiomyocytes were counted using a hemocytometer (cells per ml), then seeded directly onto collagen-coated tissue culture dishes (6 well plates). For immunocytochemistry, cells were plated 325,000 per well, for qPCR 500,000 per well. Cells were then recovered overnight in DMEM growth medium in an incubator at 37 °C with 5% CO2. The next day, DMEM growth medium was replaced with serum-free (SF) medium and incubated for another day (up to 24 h) at 37 °C prior to conducting specific experiments.

2.3 NEONATAL RAT CARDIOMYOCYTE TREATMENTS

To induce hypertrophy, cardiomyocytes were treated for 1, 3, 6, 12, and 24 hours with the following hypertrophic agonists diluted in Serum-Free control medium (SF, Control): hCT1 recombinant protein at 0.5 nM (10 ng/ml) and PE at 100 uM. Serum-free control medium was also used as a non-hypertrophic control.

For MARK2 inhibition, cardiomyocytes were pre-treated with N-(2,5-Dimethylphenyl)-2-(4-(4-methoxyphenyl)-3-oxo-3,4-dihydropyrazin-2-ylthio)acetamide (MARK/Par-1 Activity Inhibitor, 20 uM; Millipore Sigma) in dimethylsulfoxide (DMSO) for 6 hours before the induction of hypertrophy when fresh inhibitor was added.

2.4 IMMUNOCYTOCHEMISTRY

Fluorescent cell staining was conducted on primary rat cardiomyocytes (or cardiac fibroblasts) that were seeded at a density of 3.25×10^5 cells directly onto 25 mm diameter collagen-coated glass coverslips. Cells were washed three times in phosphate-buffered saline (PBS) (3 min each) followed by fixation in ice-cold methanol for 10 mins. Cells were then permeabilized in blocking buffer (5% bovine serum albumin – BSA, 2% normal goat serum, 0.4% Tx-100 in PBS) for 15 min. Cells were then incubated for 1 h at room temperature with primary antibody (diluted in blocking buffer) followed by three successive washes in PBS at 5 min each. Cells were then blocked again for 15 min followed by a 1 h incubation in fluorescently conjugated secondary antibody (diluted in blocking buffer). Cells were then washed in PBS (five times at 5 min each). Nuclei were counterstained with 4’,6-diamidino-2-phenylindole (DAPI) for 10mins and cells were mounted onto microscope slides with DakoCytomation fluorescent mounting medium (Dako). Digital fluorescent images were obtained using the Zeiss AxioVision SE64 Imaging software.

Primary antibodies used: mouse anti-α-actinin (A7811;Sigma) 1:400, rabbit anti-MARK2 (#9118;Cell Signal)1:200, Anti-Tau (phosphoS262) antibody(ab131354;abcam) 1:100, α-Tubulin (#2144; Cell Signal) 1:100. Secondary antibodies used: Alexa Fluor-488 goat anti-rabbit 1:1000 and Alexa Fluor-647 donkey anti-mouse (ThermoFisher) 1:1000. Nuclei were counterstained with DAPI as above. Fluorescent images were collected using the Zeiss Observer Z1 light microscope and using Zeiss AxioVision SE64 Imaging software. Analysis of fluorescent images performed using ImageJ.

2.5 SMALL INTERFERING RNA KNOCKDOWN

Primary cardiomyocytes were transfected using TransIT-TKO® Transfection Reagent (Mirus), serum-free Opti-MEM a (Gibco), and MARK2 small interfering RNA (siRNA)(Invitrogen) or negative control scrambled siRNA (Invitrogen) for 5 hours at 37°C with 5% CO2. The medium was replaced with serum-free medium, and cells were incubated overnight at 37°C with 5% CO2. The following day, cardiomyocytes were treated with hypertrophic stimuli treatments and appropriate controls.

2.6 CELL AREA AND FLUORESCENCE ANALYSIS

Measuring cell area was performed using ImageJ. Selection of cell area was performed with drawing/selection tools and the area was recorded as measurement. See Appendix Figure 1. Length and width measurements were recorded by drawing a line across the greatest length and width sections of the cell then recorded to determine length and width ratio.

Measuring cell fluorescence was performed using ImageJ. Area of interest was used with drawing/selection tools. Determining the level of cellular fluorescence as calculated using the

Corrected Total Cell Fluorescence (CTCF) formula. CTCF = Integrated Density – (Area of selected cell X Mean fluorescence of background readings).

2.7 STATISTICAL ANALYSIS

All data are expressed as mean ± standard error of the mean (SEM). Statistical significance for multiple-group comparisons was determined using one-way ANOVA followed by post-hoc statistical analysis (GraphPad Prism software). Tukey's test was used for pairwise comparisons between treatment groups. $p < 0.05$ was considered significant.

CHAPTER 3: RESULTS

3.1 TOTAL MARK2 EXPRESSION IS ALTERED IN NRVMS DURING PATHOLOGICAL HYPERTROPHY.

This study aims to investigate the localization and role of MARK2 in cardiomyocytes under pathological and physiological cardiac hypertrophy. Despite the critical involvement of MARK2 in cell polarity and maintaining microtubule dynamics, there is a lack of research on whether this kinase alters similar features in cardiomyocytes. We freshly isolated neonatal rat ventricular myocytes and treated them with phenylephrine (PE) at 100 μM, an α-adrenergic agonist, to induce pathological hypertrophic remodeling or cardiotrophin 1 (CT1) at 0.5 nM (10 ng/ml) to induce physiological remodeling, while serum-free media was used as a control. In previous experiments conducted by our laboratory, we have shown that both PE and CT1, a cytokine, can induce either adverse or beneficial remodeling of the heart, where CT1 engages essential characteristics of physiological hypertrophy and pro-vascular paracrine signaling in the cardiomyocyte population [137]. The NRVMs were treated for 24-hours to observe the full development of hypertrophic remodeling in the majority of myocytes as we have noted above [137]. Using immunofluorescence (IF), we observed that under serum-free untreated conditions, MARK2 congregates mainly around the perinuclear area of NRVMs (Figure 3.1A). However, following a 24-hour treatment with PE, the MARK2 protein in NRVMs disperses and is no longer centralized around the perinuclear area (Figure 3.1B). In contrast, under physiological remodeling induced by CT1 treatment, MARK2 protein has a more dispersed pattern with a perinuclear concentration and diffuse cytoplasmic localization **(**Figure 3.1B). Image analysis of fluorescent intensity of total MARK2 immuno-staining in NVRM treatments indicated that there is a significant increase in total MARK2 signal with cells undergoing pathological remodelling in comparison to control (p-value= $p < 0.05$), yet

no significant change in signal activity in NRVMs subject to physiological hypertrophy with CT1 exposure (Figure 3.1C) (p-value= $p < 0.05$).

The altered MARK2 localization with PE treatment suggests that this kinase may play a role in hypertrophic remodelling, specific to pathologic signaling events. However, it remains unclear whether MARK2 plays a role as an initiating signal for the early morphological changes associated with hypertrophy. The ability of MARK2 related kinases to modify structural elements within cardiomyocytes and the MARK2 distribution observed in the present experiments suggests that MARK2 is a probable candidate to modify early hypertrophy related cell adaptations. For example, microtubules can undergo rounds of growth and retraction over a time scale of minutes to hours which is consistent with the 24-hours alteration in MARK2 localization in response to PE. Therefore, we characterized the temporal pattern of MARK2 distribution during hypertrophic remodelling of cardiomyocytes, at 0, 1, 3-, 6-, 12-, and 24-hours following PE or CT1 administration (Figure 3.2A-B). Interestingly, MARK2 expression, as measured by IF analysis, demonstrated a significant increase (p-value= $p < 0.0001$) within the first 3 hours of pathological remodelling in PE-treated NRVMs and declined at 12- and 24-hour timepoints **(**Figure 3.2C). A smaller increase in expression of MARK2 was observed in NVRMs undergoing physiological remodelling stimulated by CT1 which peaked around 12 hours and declined at subsequent time-points.

A

Control

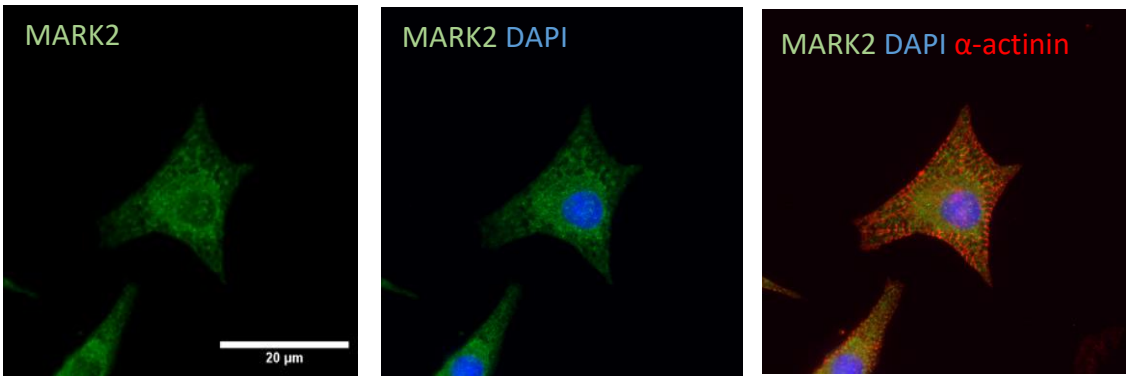

B **(24 hour hypertrophic stimuli)**

PE (100uM)

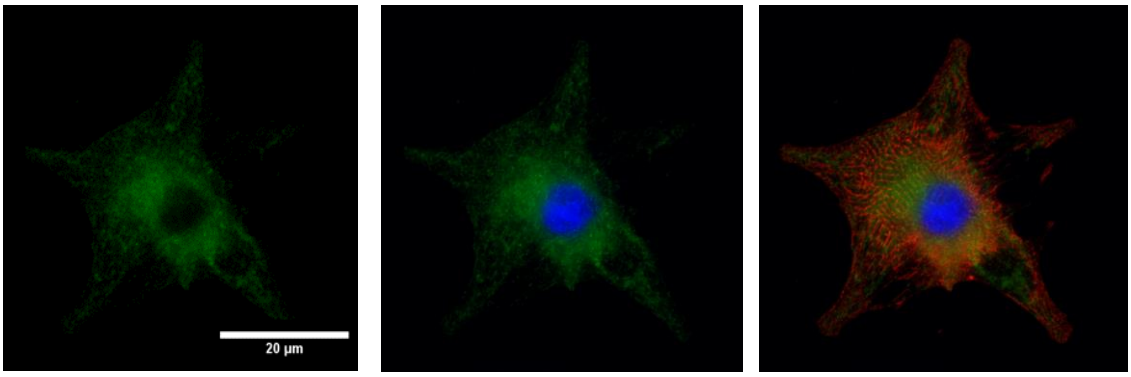

hCT1 (10nM)

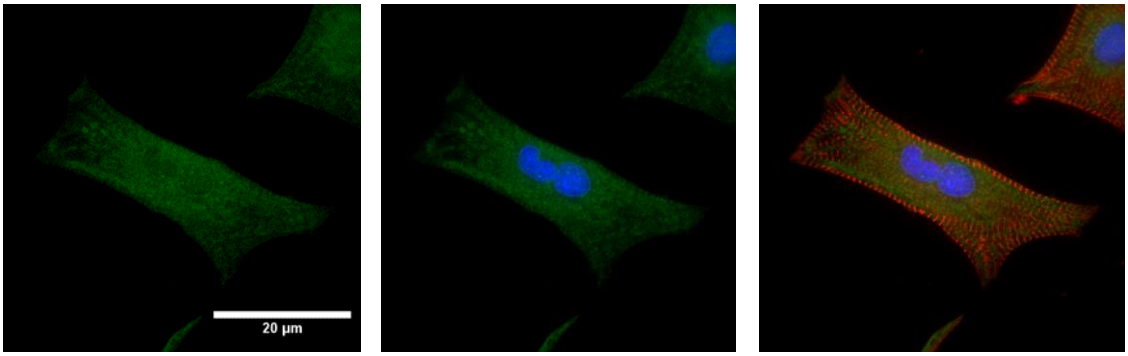

C

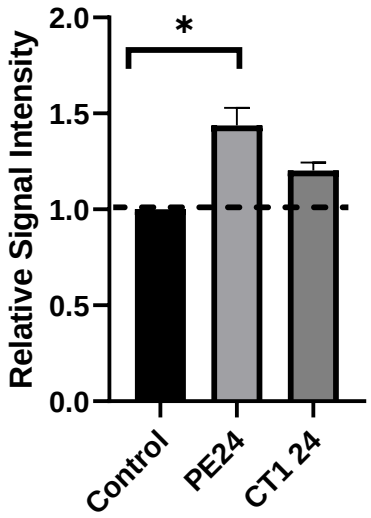

Figure 3.1. Total MARK2 localizes primarily in the perinuclear area of neonatal cardiomyocytes. NVRMs were treated with serum-free medium (Ctrl)**(A)**, PE (100 μM) **(B)**, and hCT1 (0.5 nM) **(B)** for 24 hour hours. Immunofluorescence was used to detect α-actinin (red), MARK2(green), and nuclei were stained with DAPI(blue). DAPI indicates 4',6-diamidino-2-phenylindole. All data are expressed as mean ± SEM. 30 cells per group were used for analysis. *$p < 0.05$, N=3. Scale Bar=20μm

A

PE (100uM)

1 hour

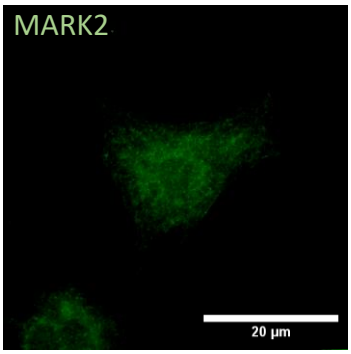

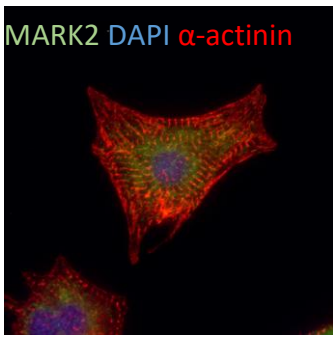

12 hours

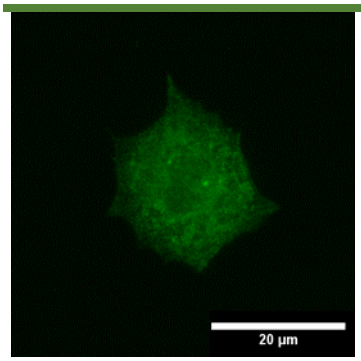

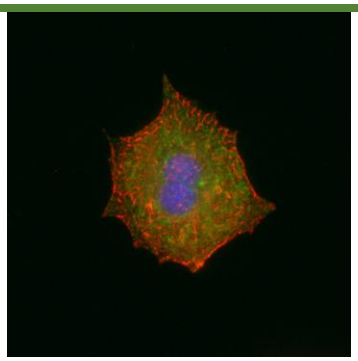

3 hours

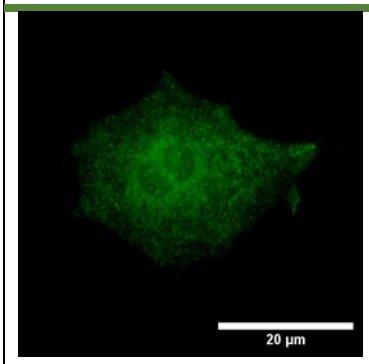

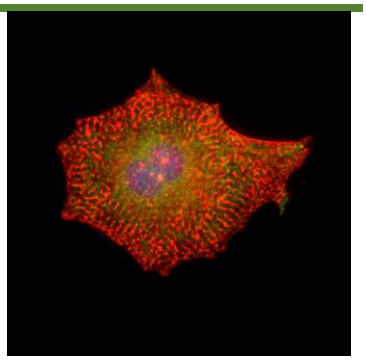

24 hours

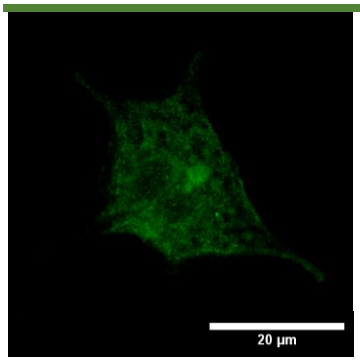

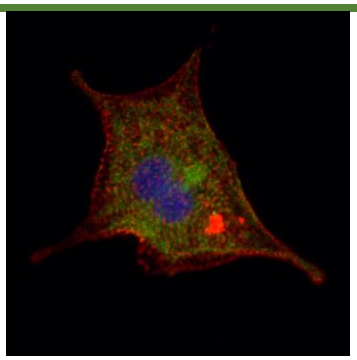

6 hours

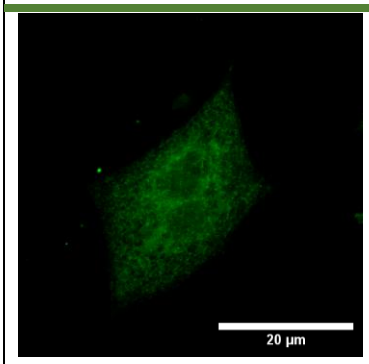

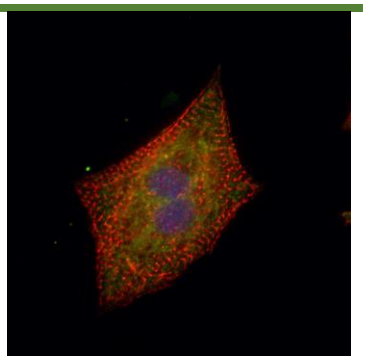

B

hCT1 (10nM)

1 hour

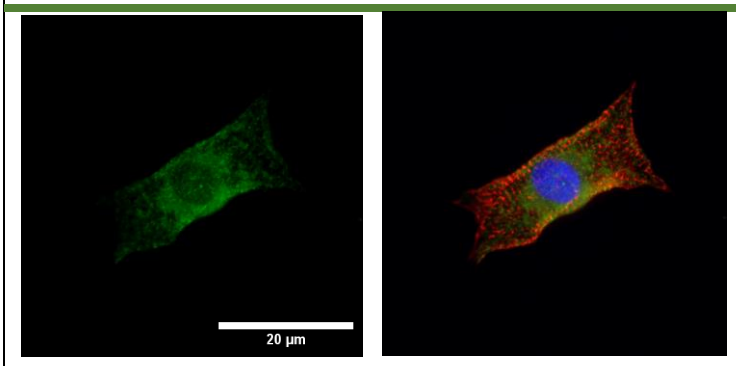

12 hours

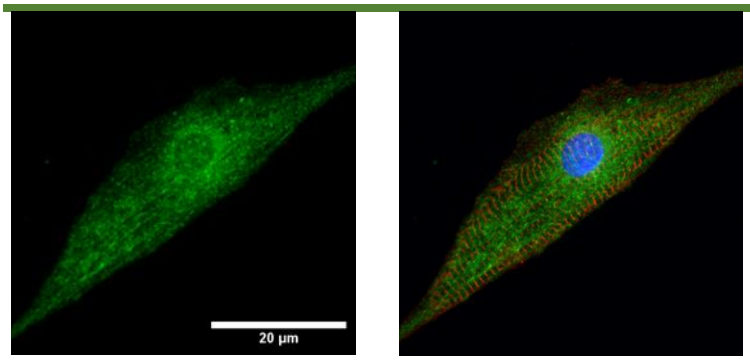

3 hours

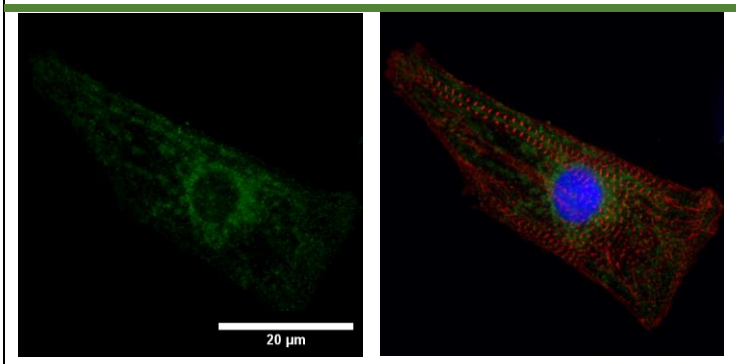

24 hours

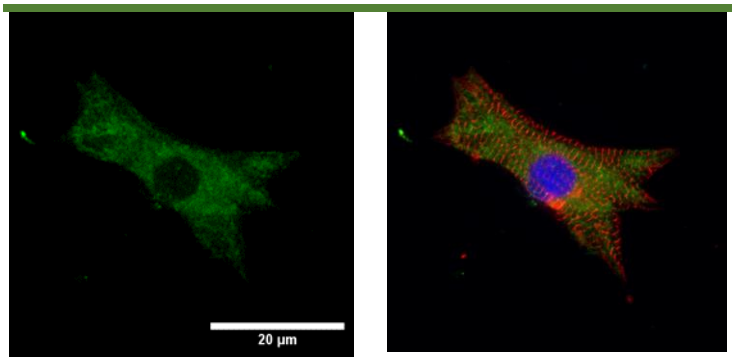

6 hours

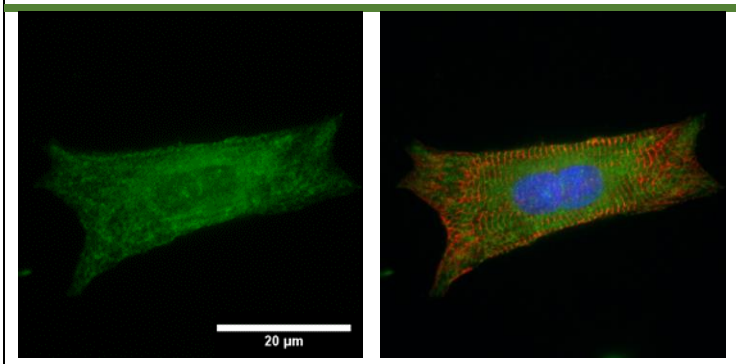

C

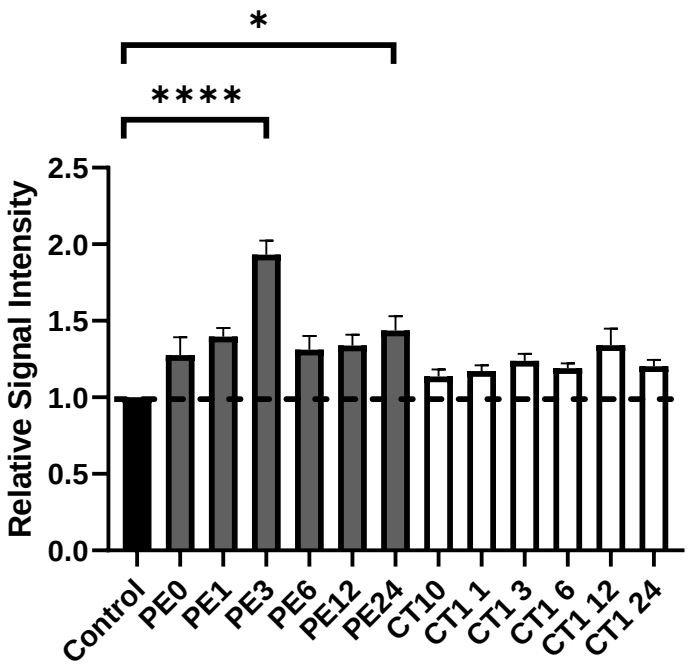

Figure 3.2. Total MARK2 expression in pathological and physiological remodelling. Primary neonatal cardiomyocytes were treated with serum-free medium (Control), PE (100 μM)**(A)**, and hCT1 (0.5 nM)**(B)** and at times 1,3,6,12, and 24 hours followed by fluorescent signal analysis. Immunofluorescence was used to detect α-actinin (red), MARK2(green), and nuclei were stained with DAPI(blue). **(C)** Quantification of MARK2 fluorescent signal as performed with ImageJ. All data are expressed as mean ± SEM. 25 cells per group were used for analysis *$p < 0.05$, ****$p < 0.0001$ N=3. Scale Bar= 20μm.

3.2 MARK2 INFLUENCES THE STRUCTURAL ALTERATIONS IN PATHOLOGICAL HYPERTROPHY.

Having determined that MARK2 localization is altered during the early morphological changes of pathological cardiac hypertrophy, we sought to determine whether MARK2 activity directly impacts cell structure/cell size in this form of adverse remodeling. To examine this question, we used a MARK2 kinase activity inhibitor 39621 (20µM; DMSO) that impairs MARK2 capacity to phosphorylate Tau. This inhibitor works as an ATP-competitive inhibitor by targeting the ATP-binding pocket to inhibit the catalytic activity of MARK2 and preventing phosphorylate Ser262 within KXGS motifs of the microtubule binding domain within Tau. Use of this inhibitor has been shown to effectively block Tau Ser262 phosphorylation in primary rat cortical neuron axon and prevent MARK2 overexpression-induced cytotoxicity in Chinese hamster ovary cells [138]. To ensure MARK2 disruption was established prior to the onset of hypertrophy signaling we pretreated NRVMs with the MARK2 inhibitor for 6-hours then exposed the cells to 24-hour hypertrophic stimuli. Image analysis of MARK2 inhibitor treatment followed by PE induced pathological remodelling induction of NRVMs indicated a failure to increase cell area, similar to the dimensions of untreated control cells (Figure 3.3). For example, a significant change was observed between cells undergoing pathological remodelling verses cells undergoing MARK2 inhibition followed by pathological stimuli (p-value=$p<0.01$). Interestingly, the inhibition of MARK2 in NRVMs during CT1 induced physiologic remodeling did not impact the increases in cell area and length-to-width ratio that occurs in response to CT1 treatment (p-value=$p<0.05$). These results suggest that MARK2 may influence the spatial growth of NRVMs in response to pathological signals but have little to no effect on the physiological remodeling of cardiomyocytes.

To verify the results observed with the MARK2 inhibitor, we also performed a siRNA mediated repression of MARK2 expression and asked whether this method would similarly disrupt the structural alterations concurrent to pathological remodeling. NRVMs were transfected via lipofectamine containing siRNA constructs during serum-free treatment of cardiomyocytes, prior to PE mediated hypertrophic-induction (Figure 3.4A-B). Similar to the effect of the MARK2 inhibitor, the siRNA mediated repression of MARK2 in PE-treated cells indicated cell area and length-to-width ratio similar to untreated control cells (p-value=$p<0.05$). Quantitative-PCR was performed to validate knockdown of MARK2 in NVRMs (Figure 3.4C). Together these observations suggest that repression of MARK2 expression or activity limits the ability of cardiomyocytes to undergo the structural alterations that result from pathological hypertrophy stimuli.

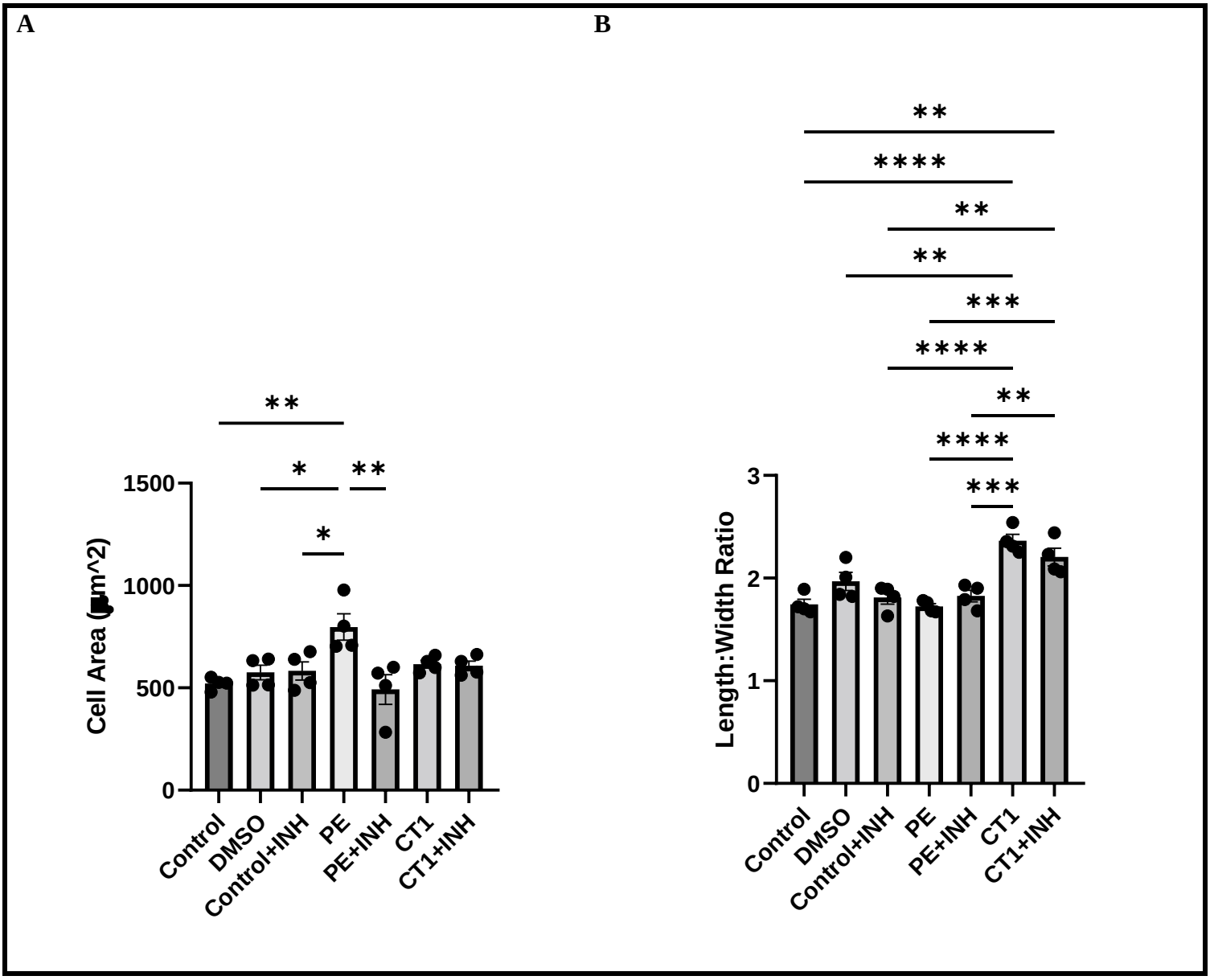

Figure 3.3. MARK2 affects the morphological structure of cardiomyocytes in pathological hypertrophy. Primary neonatal cardiomyocytes stimulated were either pretreated with MARK2 kinase activity inhibitor 39621 (20µM; DMSO) followed by either 24 h with phenylephrine (PE), α-adrenergic agonist (100 µM), and human cardiotrophin 1 (hCT1) (0.5 nM), or control serum-free medium (Ctrl) followed by morphometric analysis. Quantification of the average cell surface

area**(A)** and length:width ratio **(B)** determined via imageJ and all data are expressed as mean ± SEM. 60 cells per group were used for analysis. Scale Bar=20µm *p < 0.05, **p < 0.01, ***p < 0.001,****p < 0.0001) N=4

A

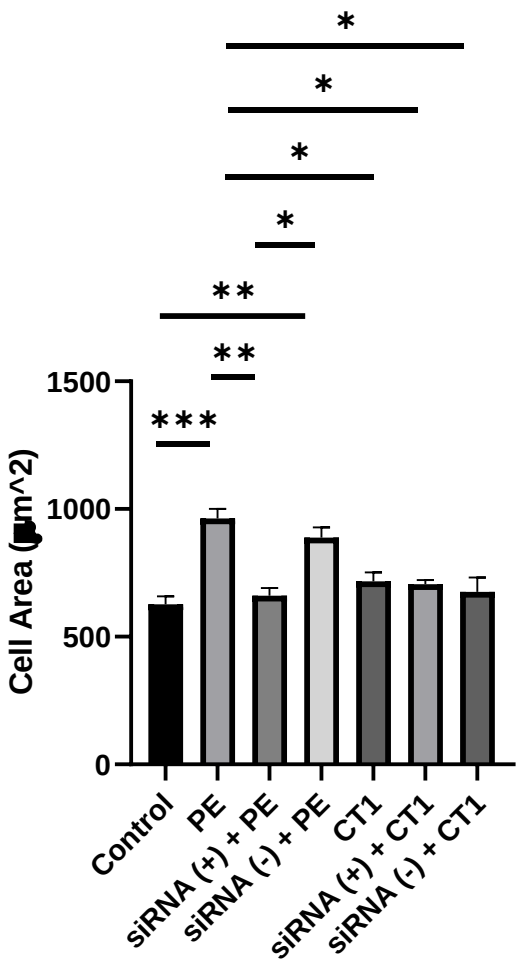
*
*
*
*
**
**
***
1500
1000
500
0
Cell Area (µm^2)
Control
PE
siRNA (+) + PE
siRNA (-) + PE
CT1
siRNA (+) + CT1
siRNA (-) + CT1

B

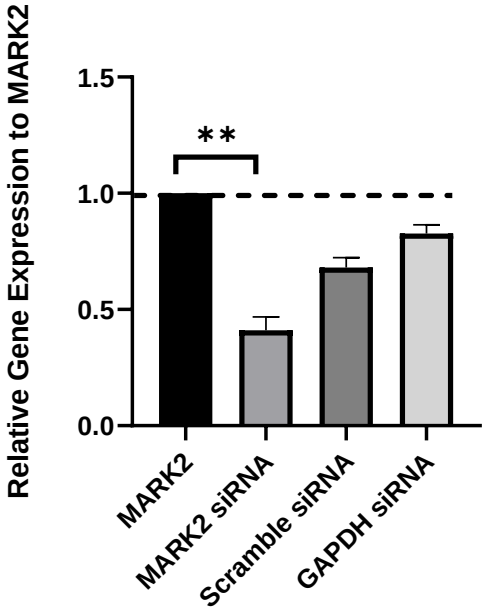

Figure 3.4. Verification of MARK2 effect on the morphological structure of cardiomyocytes in pathological hypertrophy. Primary neonatal cardiomyocytes were either treated with siRNA MARK2 or negative control via TransIT-TKO transfection reagent followed by 24hour recovery and stimulation for 24 h with phenylephrine (PE), α-adrenergic agonist (100 μM) or control serum-free medium (Ctrl) followed by morphometric analysis. Quantification of the average cell surface area and length:width ratio determined via imageJ and all data are expressed as mean ± SEM**(A)**. MARK2 knockdown confirmed by qPCR, where MARK2 siRNA led to reduced MARK2 levels compared with the control normal MARK2, negative scrambled siRNA, and GAPDH siRNA**(B)**.*$p < 0.05$, **$p < 0.01$, ***$p < 0.001$. N=3

3.3 MARK2 IMPACTS ON MICROTUBULE DENSITY.

Having established that the inhibition of MARK2 does affect the activity of pTauS262, we wished to examine the downstream effects of the inhibitory capacity of MARK2 in cardiac hypertrophy. One of the major roles of Tau is acting as microtubule associated protein (MAP) to influence the stability of microtubules of the cytoskeletal structure of the cell. More importantly, previous studies have shown that the density of the microtubule network increases significantly in end-stage heart failure of diverse etiology [139,140]. As a result, we wish to determine whether the inhibition of MARK2 affects cardiac hypertrophy morphology be affecting the microtubule network. Performing an immunofluorescence, we observed an increase in microtubule density in pathological remodelling NVRMs in comparison to untreated control, especially around the perinuclear area of the cell (Figure 3.5A-B). With the addition of the MARK2 inhibitor, we see a decrease in microtubule density of NVRMs followed with pathological hypertrophic stimuli. Similar results were seen with siRNA knockout of MARK2 in NVRMs.

A

Control	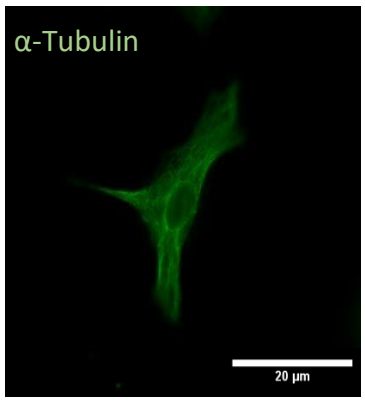	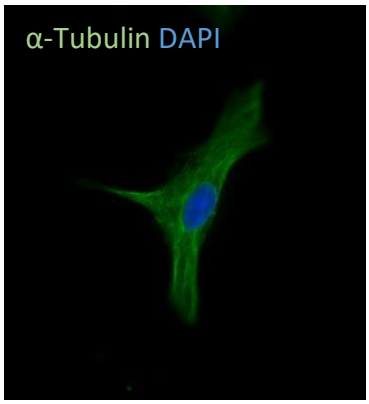	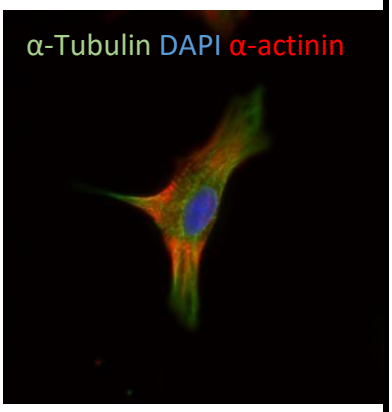
PE (100uM)	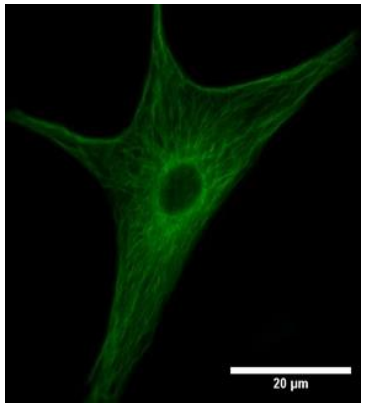	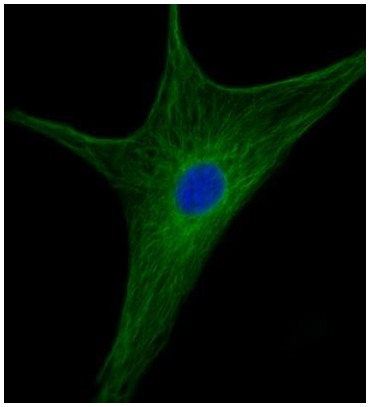	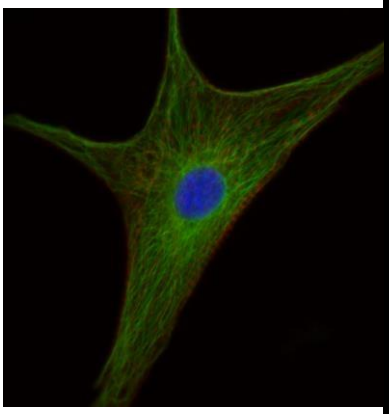
PE (100uM)+ MARK2 Inhibitor	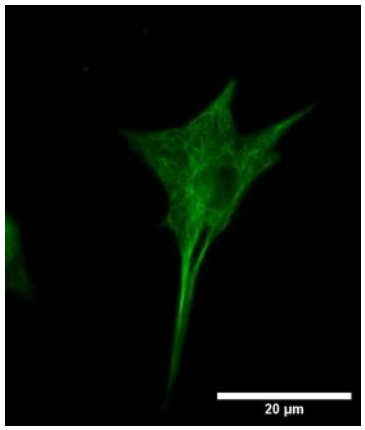	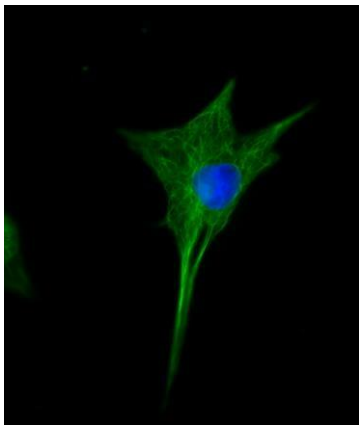	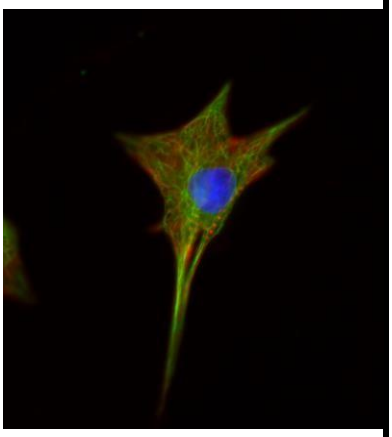

PE +

MARK2 (+)siRNA

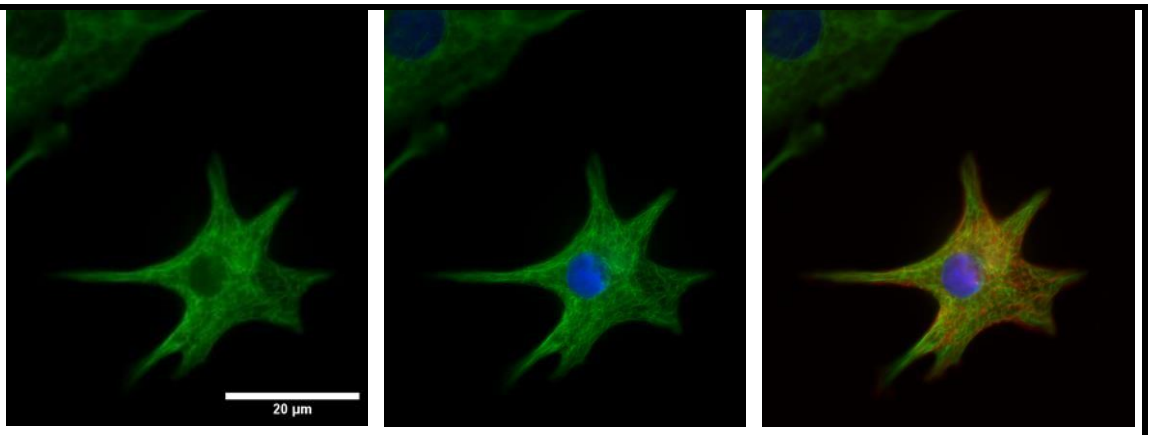

B

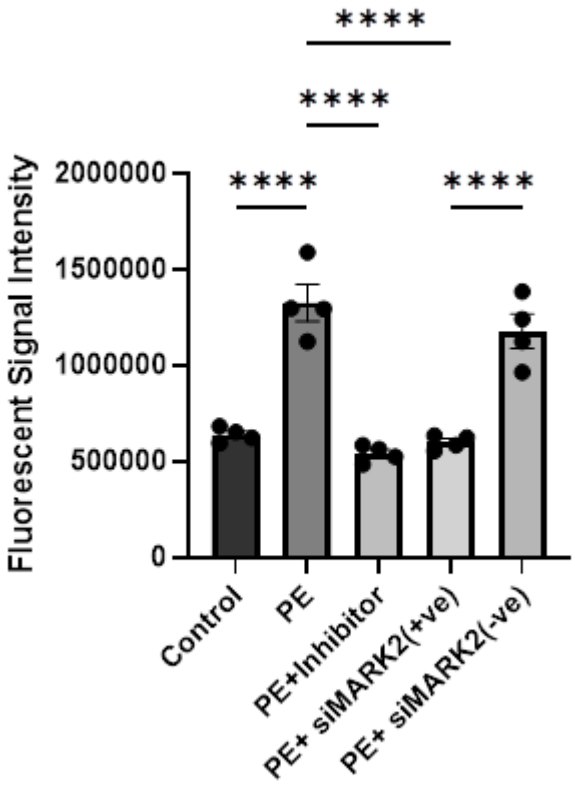

Figure 3.5. MARK2 affects microtubule activity pattern in pathological cardiac hypertrophy. Primary neonatal cardiomyocytes stimulated were either pretreated with MARK2 kinase activity inhibitor 39621 followed by 24 h with phenylephrine (PE) or control serum-free medium (Control). NVRMs were also treated with siRNA MARK2 or negative control via TransIT-TKO transfection reagent followed by 24hour recovery and stimulation for 24 h with phenylephrine (PE), α-adrenergic agonist (100 μM). Immunofluorescence was used to detect α-actinin (red), α-Tubulin (green), and nuclei were stained with DAPI(blue)**(A)**. DAPI indicates 4',6-diamidino-2-phenylindole. Quantification of α-tubulin fluorescent signal as performed with imageJ**(B)**. All data are expressed as mean ± SEM. 25 cells per group were used for analysis. Scale Bar=20μm ****$p < 0.0001$ N=4

3.4 INHIBITION OF MARK2 EFFECTS ACTIVITY OF TAU AT SERINE262.

We also wished to validate whether the MARK2 inhibitor does affect the phosphorylation of Tau at Serine262 (pTauS262) in NVRMs. No studies to date have observed the phosphorylation of TauSer262 in cardiomyocytes and we wish to determine if and where pTauS262 is present in NVRMs. Interestingly, studies have indicated that phosphorylation of tau at Ser262 destabilizes microtubule stability and that the stabilization of microtubule-unbound tau by phosphorylation at Ser262/356 via the MARK2 pathway may act in the initial steps of tau mismetabolism in Alzheimer's disease pathogenesis. Similar to our pervious immunofluorescence study setup, we treated NVRMs with various hypertrophic stimuli and appropriate controls followed by fixation and stained for pTauS262. Our observations indicated that in untreated NVRMS, pTauS262 activity is primarily present in the nucleus (Figure 3.6A-B). Neonatal cardiac cells under pathological cardiac hypertrophy have an increase activity of phosphorylated Tau at Serine262. siRNA knockout of MARK2 to NVRMs followed by pathological remodelling had a similar trend further validating that the inhibition of MARK2 affects phosphorylation activity of Tau at Serine262(Figure 3.6A-B).

A

Control	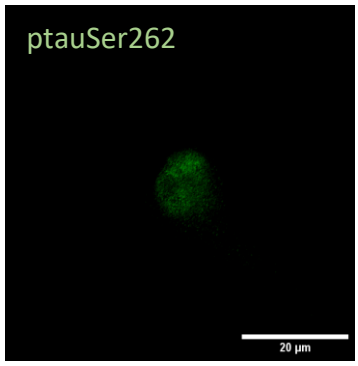	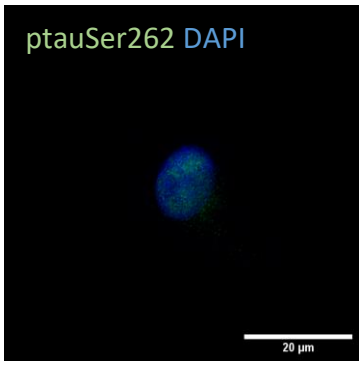	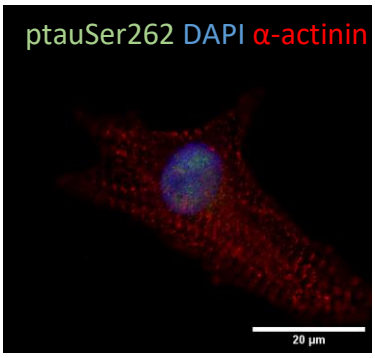
PE (100uM)	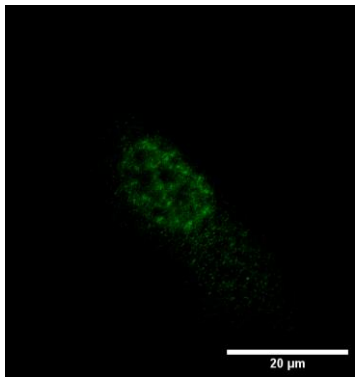	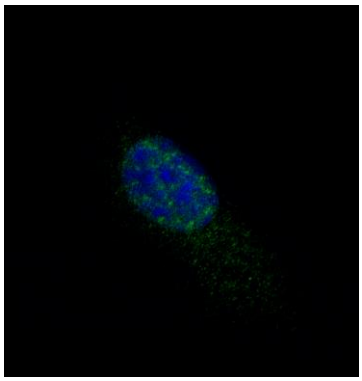	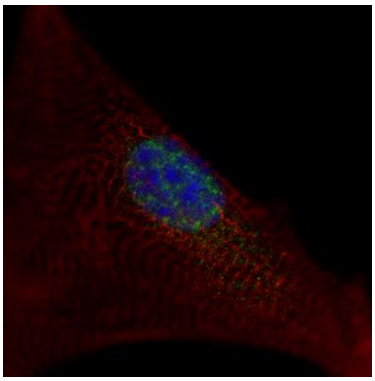
PE (100uM)+ MARK2 INH(20µM)	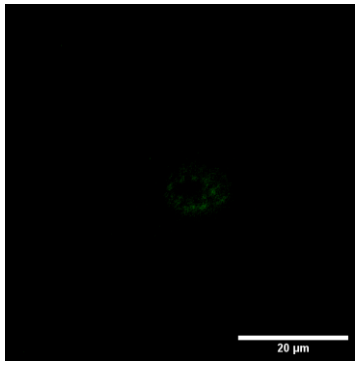	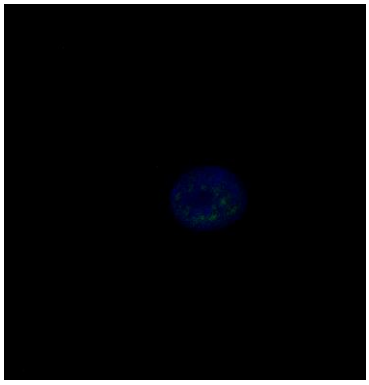	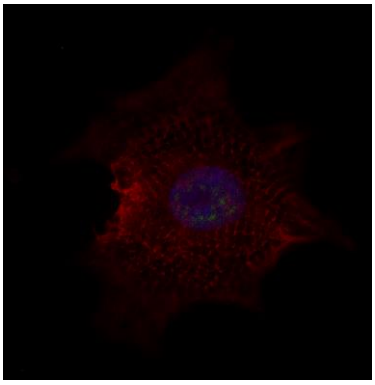
PE + MARK2(+)siRNA	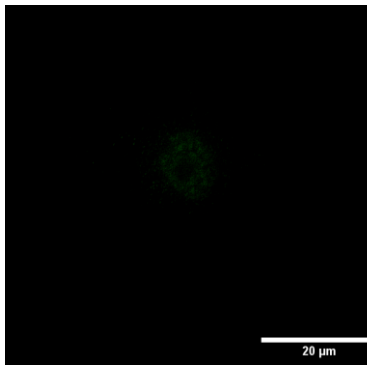	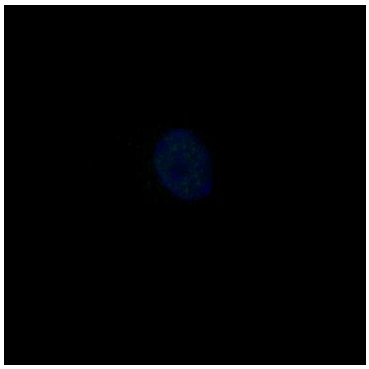	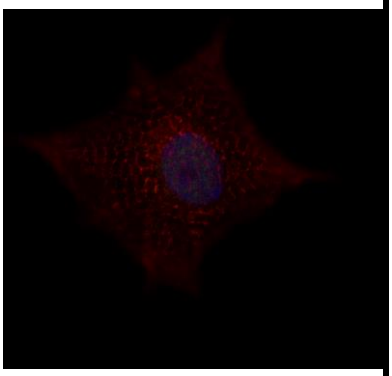

PE +

(-)siRNA

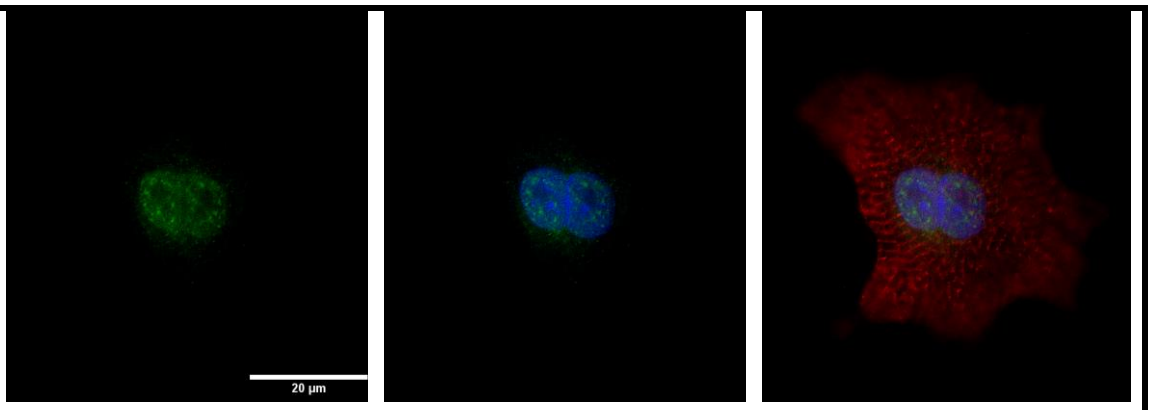
20 µm

B

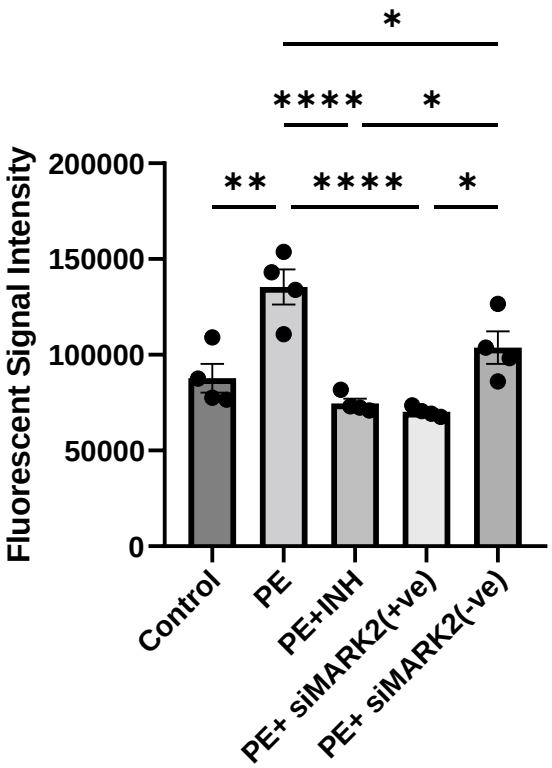
*
****
*
**
****
*
Fluorescent Signal Intensity
200000
150000
100000
50000
0
Control
PE
PE+INH
PE+ siMARK2(+ve)
PE+ siMARK2(-ve)

Figure 3.6. MARK2 affects activity of phosphorylated site Serine262 on Tau in pathological hypertrophy. Primary neonatal cardiomyocytes stimulated were either pretreated with MARK2 kinase activity inhibitor 39621 followed by 24 h with phenylephrine (PE) or serum-free medium (Control). NVRMs were also treated with siRNA MARK2 or negative control via TransIT-TKO transfection reagent followed by 24hour recovery and stimulation for 24 h with phenylephrine (PE), α-adrenergic agonist (100 μM). Immunofluorescence was used to detect α-actinin (red), pTauSer262(green), and nuclei were stained with DAPI(blue)**(A)**. DAPI indicates 4',6-diamidino-2-phenylindole. Quantification of MARK2 fluorescent signal as performed with imageJ**(B)**. All data are expressed as mean ± SEM. 25 cells per group were used for analysis. Scale Bar=20μm *p < 0.05, **p < 0.01, ****p < 0.0001 N=4

3.5 MARK2 EFFECTS ON NUCLEOPLOIDY.

With our observations indicating MARK2 is primarily centered in the perinuclear area and that inhibition of MARK2 activity affects pTauSer262 in the nucleus, we sought to determine whether MARK2 had an effect in binucleation of NVRMs. Studies have indicated that an increased in nuclear ploidy is often observed in connection with cardiac hypertrophy [140-143]. To this end, we quantified mononucleated and binucleated NVRMs under the various hypertrophic stimuli and controls to determine whether MARK2 may have an impact on binucleation. Our results indicated that there is a greater number of binucleated cardiomyocytes under pathological hypertrophy while untreated cardiomyocytes are mainly mononucleated (p value= $p < 0.0001$)(Figure 3.7). MARK2 inhibitor followed by pathological remodelling impacts binucleation of NVRMs resulting in a greater number of mononucleated cells(p value= $p < 0.0001$).

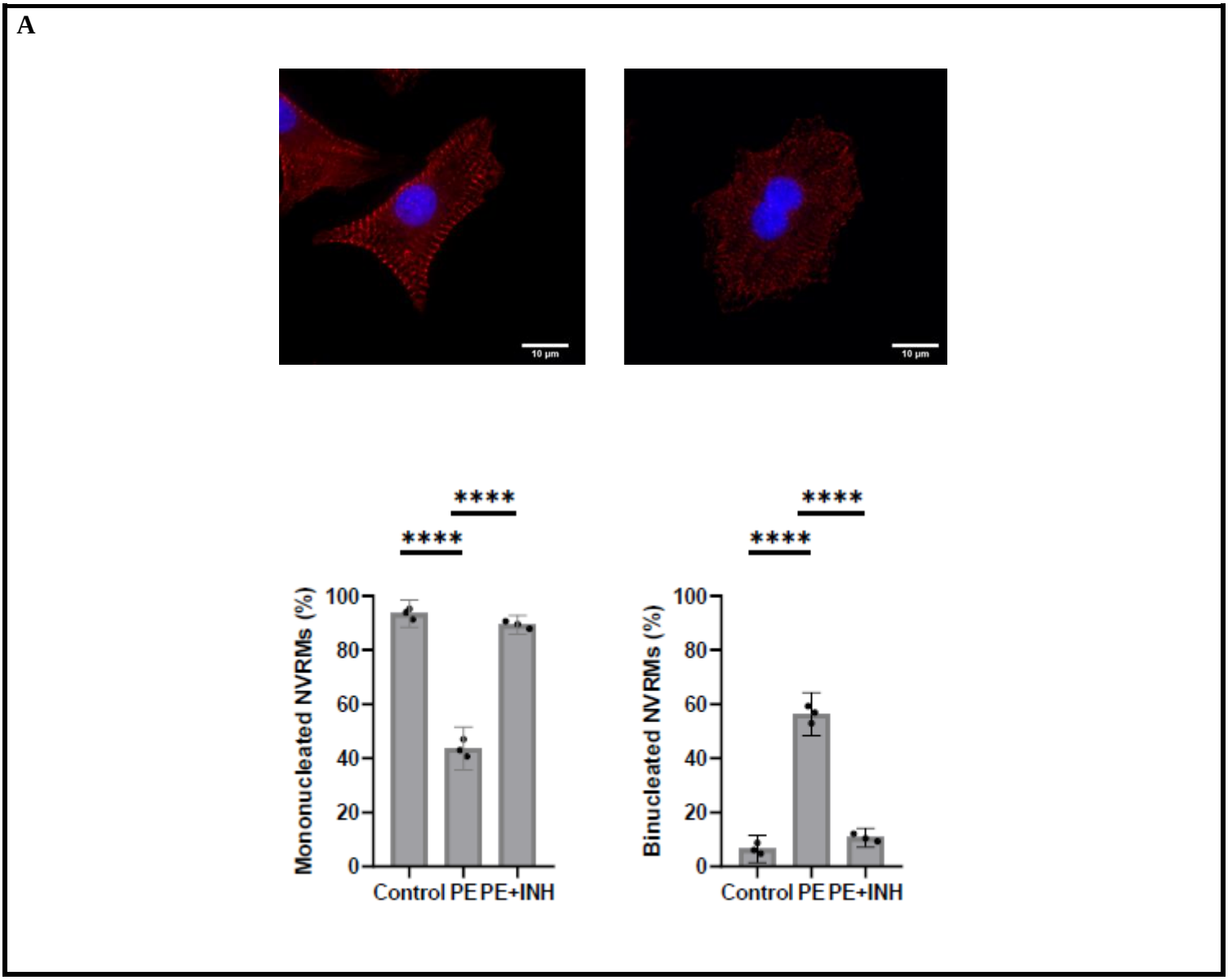

Figure 3.7. Nuclear ploidy is affected during pathological hypertrophy and MARK2 treatment. Primary neonatal cardiomyocytes stimulated were either pretreated with MARK2 kinase activity inhibitor 39621 (20µM; DMSO) followed by either 24 h with phenylephrine (PE) α-adrenergic agonist (100 µM), PE α-adrenergic agonist (100 µM) only, or control serum-free

medium (Control) followed by quantification of mononucleated and binucleated NRVMs. All data are expressed as mean ± SEM. 25 cells per group were used for analysis. ****$p < 0.0001$. N=3

CHAPTER 4: DISCUSSION AND CONCLUSION

Overall, the observations we established help to provide clarity on the role that MARK2 has in driving cytoskeleton alterations to shift cell morphology in cardiac hypertrophy. From our observations we have established four primary conclusions: 1) Total expression of MARK2 is affected in NRVWs during pathological hypertrophy and not in physiological hypertrophy. 2) MARK2 influences the structural alterations of NRVMs seen in pathological hypertrophy. 3) MARK2 influences the activity of Tau at Serine262 and microtubule density in NRVMs. 4) Nuclear ploidy is affected during pathological hypertrophy and MARK2 treatment.

At this stage, we have identified MARK2's role in affecting the growth of cardiomyocytes in the early morphological changes associated with pathological cardiac hypertrophy. How extensive MARK2's influence is with regard to the full development of pathological and physiological hypertrophy has yet to be determined.

4.1 MARK2 STRUCTURAL ALTERATIONS IN CARDIOMYOCYTES

While the importance of MARK2 is established in neurons, there is a lack of research on its capacity to affect cytoskeletal organization in cardiomyocytes. We performed immunofluorescent imagery to provide a better understanding of total expression of MARK2 within NRVMs and its localization. We first determined that MARK2 primarily congregates in the perinuclear region of NRVMs in our control untreated group. Interestingly, microtubules located around the cell nucleus in cardiomyocytes are amongst the most stable in this cell lineage, even resisting treatments with colchicine or nocodazole [75,144]. However, little information is available regarding the mechanisms that stabilize these types of microtubule networks and how this imparts functionality to the cardiomyocyte.

To our surprise, following a 24-hour exposure to pathological hypertrophic stimuli, the MARK2 protein in NRVMs disperses and is no longer concentrated around the perinuclear region. While under physiological remodeling, the MARK2 signal centralizes around the perinuclear area similar to that of untreated control cells. These findings suggest that MARK2 might play a key step that allows for the expansion of the cardiomyocyte in response to pathological hypertrophy remodelling. Additionally, the MARK2 inhibitor impacted the growth of pathological and not physiological remodelling. Therefore, we propose that inhibition of MARK2 stalls pathological remodelling and that the dispersion of MARK2 in a cardiomyocyte is necessary to allow for physiologic adaptation/growth of the cell. We propose that MARK2 might contribute to the organization of perinuclear organelles or engage with the microtubule-organizing centers (MTOCs) located in the perinuclear area, facilitating its interaction. The MTOC provides spatial and temporal control over the initiation of microtubule growth, and interestingly MARK2 has been known to promote both MTOC orientation and leading-edge MT growth [145,146]. More importantly, among the family of MARKs, MARK4 has been recognized to be directly involved in microtubule organization by binding to the MTOC and to nucleating microtubules as well as regulating the correct positioning of MTOC [147].

In addition, we showed an increase in the total expression of MARK2 during pathological cardiomyocyte hypertrophy but not in an in vitro model of physiological hypertrophy. A reasonable conclusion to be drawn from this observation is that MARK2 expression/activity is conducive to the promotion of negative remodeling events within the affected cardiomyocyte population. How MARK2 achieves this outcome is not conclusive, however our observations are consistent with this kinase affecting cytoskeletal elements, which in turn provide the structural support for the negative remodeling event. For example, numerous studies have demonstrated

rapid alterations in the density and configuration of the microtubular and intermediate filament network specifically in pathological cardiac hypertrophy [88,92,139]. These swift modifications impact the density, dynamics, and binding partners of the microtubule network, particularly in heart failure [75]. As noted before, the response of myocytes from pressure-overloaded versus volume-overloaded heart differs significantly [2].

However, it is known that the accumulation of a dense network of microtubules can lead to interference with physiological function, ultimately resulting in contractile dysfunction of the cardiomyocytes [87,88,91,92,149]**.** This outcome, distinct from physiological hypertrophic growth, underscores the intricate consequences of these microtubular alterations. For example, Cooper and colleagues in a previous study have shown that feline volume-overload hypertrophy fails to alter microtubule density or cardiomyocyte function despite an increase in right ventricular chamber size [149]**,** a model equivalent to physiologic hypertrophy. While other studies have established an increase in the amount of tubulin in cardiomyocyte dysfunction observed in pressure-overload hypertrophy [87,88,91,92], which is more akin to a pathologic model of cardiac hypertrophy. In addition to MARK2, other MARK kinases have been implicated in heart failure phenotypes. MARK4 has been shown to influence heart failure by alternating cardiomyocyte contractility through the modulation of microtubule detyrosination in the failing heart [150].

Clearly, the fact that MARK2 is expressed in healthy cardiomyocytes suggests that this kinase may retain basal activity that promotes normal cell function. The corollary to this hypothesis would suggest that any dramatic increase or decrease in MARK2 function would elicit a pathologic response in any affected cell, including cardiomyocytes. Such a rheostat function for MARK2 has been revealed in the study of murine models of Duchenne Muscular Dystrophy, where the absence of dystrophin in activated muscle stem cells causes the expression of MARK2 to be

downregulated, resulting in the inability manage cell polarity with PAR-3 in this cell type [151]. In turn, this loss of polarity control leads to an inability of the dystrophic stem cell population to engage asymmetric cell division, which is the key step in the production of the differentiation competent daughter cell and the eventual repair of the damaged muscle fiber [151]. Given, this overt impact on muscle stem cell polarity, it is tempting to speculate that MARK2 may also exert similar polarity controls within cardiomyocytes, that in turn impact the hypertrophy response. Interestingly, loss of dystrophin is coincident with a transition from compensated pathologic hypertrophy to heart failure, suggesting the concurrent loss of MARK2 may act as the molecular switch that destabilizes the microtubular structure of dystrophic cardiomyocytes. This event alone may make the dystrophic cardiomyocyte prone to stress related cues that govern hypertrophy, acting in concert with the structural deficits that result from the loss of dystrophin itself.

4.2 MARK2 EFFECT ON TAU SERINE 262 AND NUCLEAR PLOIDY

Having established that MARK2 does impact pathological cardiomyocyte hypertrophy, we wished to determine the mechanism by which this kinase controls this pathologic cell size adaptation. Prior studies have confirmed that MARK2 phosphorylates and modifies tau activity in neurons, a signaling event that is hypothesized to initiate neuron dysfunction in Alzhemier's disease, a pathology that is also characterized by microtubule derangement [116,152,153]. To address whether MARK2 induced cardiomyocyte pathology via tau, we examined whether the known MARK2 Ser262 phosphorylation site in the tau protein was altered when MARK2 activity was inhibited. To our surprise, we observed the phosphorylation of Tau at Ser262 in untreated NRVMs was localized in the nucleus and perinuclear region, with an increased phosphorylation signal during PE induced pathological hypertrophy.

Interestingly, prior studies have indicated that a nuclear form of tau has been found to co-localise with the pericentromeric heterochromatin and with key nucleolar proteins like nucleolin to play a role in chromosome stabilization and regulate transcription [154,155]. It also appears that Tau mutations appear to alter chromosome stability, while tau pathology induces chromatin relaxation [156,157]. Given our understanding of tau in and surrounding the nucleus, albeit limited, we postulate that MARK2 might be phosphorylating Tau at Ser262 to alter chromosome stability and transcription regulation in and around the nucleus. This could potentially yield supplementary transcriptional output to facilitate protein biosynthesis for cell growth during pathological hypertrophy. However, a comprehensive investigation is necessary to precisely ascertain the role of MARK2 and pTauSer262 within the nucleus.

In addition, our results reveal an increased occurrence of binucleated cardiomyocytes during pathological hypertrophy that is sensitive to the activity and expression of MARK2, whereas untreated cardiomyocytes are predominantly mononucleated. This observation suggests that MARK2 and pTauSer262 may influence the nuclei/ploidy status in cardiomyocytes. Multinucleation in cardiomyocytes often arises from acytokinetic mitosis, commonly referred to as failed cytokinesis [27]. Previous studies have proposed that this outcome stems from an anomalous distribution of mitotic microtubules, which in turn disrupts the effective anchoring of the actomyosin ring to the plasma cell membrane [158,159]. Both RhoA and Tau have been shown to be instrumental in upholding microtubule stability and facilitating the anchorage of the actomyosin ring to the plasma cell membrane [159], while the mislocalisation of these same proteins cause cytokinesis failure allowing for binucleation in the single cell to occur . Further experiments should focus on whether MARK2 acts directly on Tau and RhoA, to moderate the development of

binucleation/ploidy, which is known to be a defined morphologic feature of pathological cardiac hypertrophy.

4.3 LIMITATIONS

Some limitations of this study include the lack of MARK2 isoform data available in NRVMs. Given that there are multiple alternative splice isoforms of MARK2 in different species, how each MARK2 isoform may contribute to induction of pathological cardiac remodelling remains unclear. Future studies examining the alternative isoforms of MARK2 and their respective targets should be undertaken to determine how this kinase elicits pathologic cardiomyocyte growth.

Another limitation in the present study is whether adult cardiomyocytes respond to MARK2 signaling events similar to what has been observed in the NRVM model. This is an important issue when attempting to attribute cause and effect for MARK2 in an adult disease pathology such as pathologic cardiac hypertrophy.

4.4 FUTURE DIRECTIONS

Our results confirm two novel observations. Firstly, we have established that the inhibition of MARK2 effects the pathological remodelling of cardiomyocytes in vitro. However, the effects of MARK2 in an in vivo model have not been performed. As a result, an in vivo experiment would help to validate MARK2 inhibitor drug as a potential therapeutic. Additionally, performing the same set of experiments on induced pluripotent stem cells human cardiomyocytes would provide insight into the effects of MARK2 as a potential therapeutic in humans.

Secondly, we have determined that MARK2 effects phosphorylation of Tau at Ser262 and nuclear ploidy in pathological remodelling. However, more work is required to study the relationship between MARK2 and development of pathological cardiac hypertrophy and heart

failure. To better understand MARK2's involvement in other molecular mechanisms associated with pathological hypertrophy, we propose using proximity labeling-based methods coupled with mass spectrometry to provide a high-throughput approach for systematic analysis of protein–protein interactions. The use of mass spectrometry will allow for an unbiased mapping of all the relevant MARK2 substrates associated with pathological hypertrophy in NVRMs including ones previous studied like HDAC4/5, aPKC complex, and RhoA [122,124-126]. These methods serve as initial discovery methods that will allow for more detailed follow-up studies. Additionally, further study is necessary to understand MARK2's involvement in the cytoskeletal structure of the cardiomyocyte to effect cardiac physiology and pathophysiology. We propose performing a cardiomyocyte contractility assay to measure contraction to determine the role that MARK2 has in effecting cardiomyocyte contractility in pathological hypertrophy.

4.5 CONCLUSION

In summary, our results show a crucial role for MARK2's role in influencing the early morphological changes seen in pathologic cardiac hypertrophy. Our observations suggest that MARK2 controls the phosphorylation of Tau at Ser262, affecting the microtubule network required for the pathologic hypertrophy of cardiomyocytes. More importantly, these findings may provide a unique potential therapeutic in preventing the progression of pathological cardiac hypertrophy and/or prevent the transition to fulminant heart failure.

REFERENCES

1) Hill, J. A. & Olson, E. N. Cardiac Plasticity. *New England Journal of Medicine* **358**, 1370–1380 (2008).
2) Pitoulis, F. G. & Terracciano, C. M. Heart Plasticity in Response to Pressure- and Volume-Overload: A Review of Findings in Compensated and Decompensated Phenotypes. *Frontiers in Physiology* **11**, (2020).
3) Berman, M. N., Tupper, C. & Bhardwaj, A. Physiology, Left Ventricular Function. in *StatPearls* (StatPearls Publishing, 2023).
4) Tan, C. M. J. & Lewandowski, A. J. The Transitional Heart: From Early Embryonic and Fetal Development to Neonatal Life. *Fetal Diagn Ther* **47**, 373–386 (2020).
5) Hillman, N., Kallapur, S. G. & Jobe, A. Physiology of Transition from intrauterine to Extrauterine Life. *Clin Perinatol* **39**, 769–783 (2012).
6) Naeije, R. & Manes, A. The right ventricle in pulmonary arterial hypertension. *European Respiratory Review* **23**, 476–487 (2014).
7) Laflamme, M. A. & Murry, C. E. Heart regeneration. *Nature* **473**, 326–335 (2011).
8) Pinto, A. R. *et al.* Revisiting Cardiac Cellular Composition. *Circ Res* **118**, 400–409 (2016).
9) Trager, L. E. *et al.* Beyond cardiomyocytes: Cellular diversity in the heart's response to exercise. *Journal of Sport and Health Science* **12**, 423–437 (2023).
10) Günthel, M., Barnett, P. & Christoffels, V. M. Development, Proliferation, and Growth of the Mammalian Heart. *Molecular Therapy* **26**, 1599–1609 (2018).
11) Santini, M. P., Forte, E., Harvey, R. P. & Kovacic, J. C. Developmental origin and lineage plasticity of endogenous cardiac stem cells. *Development* **143**, 1242–1258 (2016).

12) Paradis, A. N., Gay, M. S. & Zhang, L. Binucleation of cardiomyocytes: the transition from a proliferative to a terminally differentiated state. *Drug Discovery Today* **19**, 602–609 (2014).

13) Zhao, M.-T., Ye, S., Su, J. & Garg, V. Cardiomyocyte Proliferation and Maturation: Two Sides of the Same Coin for Heart Regeneration. *Frontiers in Cell and Developmental Biology* **8**, (2020).

14) Naqvi, N. *et al.* A Proliferative Burst during Preadolescence Establishes the Final Cardiomyocyte Number. *Cell* **157**, 795–807 (2014).

15) Kang, M. J., Kim, J. S., Chae, S. W., Koh, K. N. & Koh, G. Y. Cyclins and cyclin dependent kinases during cardiac development. *Mol Cells* **7**, 360–366 (1997).

16) Ng, D. C. H. *et al.* Centrosome Reduction Promotes Terminal Differentiation of Human Cardiomyocytes. *Stem Cell Reports* **15**, 817–826 (2020).

17) Wong, Y. L. *et al.* Reversible centriole depletion with an inhibitor of Polo-like kinase 4. *Science* **348**, 1155–1160 (2015).

18) Pasumarthi, K. B. S. & Field, L. J. Cardiomyocyte Cell Cycle Regulation. *Circulation Research* **90**, 1044–1054 (2002).

19) Singh, A., Singh, A. & Sen, D. Mesenchymal stem cells in cardiac regeneration: a detailed progress report of the last 6 years (2010–2015). *Stem Cell Research & Therapy* **7**, 82 (2016).

20) Pasumarthi, K. B. S. & Field, L. J. Cardiomyocyte Cell Cycle Regulation. *Circulation Research* **90**, 1044–1054 (2002).

21) Uygur, A. & Lee, R. T. Mechanisms of Cardiac Regeneration. *Developmental Cell* **36**, 362–374 (2016).

22) Bishop, S. P., Zhang, J. & Ye, L. Cardiomyocyte Proliferation from Fetal- to Adult- and from Normal- to Hypertrophy and Failing Hearts. *Biology (Basel)* **11**, 880 (2022).

23) Mollova, M. *et al.* Cardiomyocyte proliferation contributes to heart growth in young humans. *Proc Natl Acad Sci U S A* **110**, 1446–1451 (2013).

24) Olivetti, G. *et al.* Aging, Cardiac Hypertrophy and Ischemic Cardiomyopathy Do Not Affect the Proportion of Mononucleated and Multinucleated Myocytes in the Human Heart. *Journal of Molecular and Cellular Cardiology* **28**, 1463–1477 (1996).

25) Miko, M. *et al.* Two nuclei inside a single cardiac muscle cell. More questions than answers about the binucleation of cardiomyocytes. *Biologia* **72**, 825–830 (2017).

26) Derks, W. & Bergmann, O. Polyploidy in Cardiomyocytes. *Circulation Research* **126**, 552–565 (2020).

27) Anatskaya, O. V., Sidorenko, N. V., Beyer, T. V. & Vinogradov, A. E. Neonatal cardiomyocyte ploidy reveals critical windows of heart development. *International Journal of Cardiology* **141**, 81–91 (2010).

28) Shimizu, I. & Minamino, T. Physiological and pathological cardiac hypertrophy. *Journal of Molecular and Cellular Cardiology* **97**, 245–262 (2016).

29) Nakamura, M. & Sadoshima, J. Mechanisms of physiological and pathological cardiac hypertrophy. *Nat Rev Cardiol* **15**, 387–407 (2018).

30) Maillet, M., van Berlo, J. H. & Molkentin, J. D. Molecular basis of physiological heart growth: fundamental concepts and new players. *Nat Rev Mol Cell Biol* **14**, 38–48 (2013).

31) Takano, A. P. C., Senger, N. & Barreto-Chaves, M. L. M. The endocrinological component and signaling pathways associated to cardiac hypertrophy. *Molecular and Cellular Endocrinology* **518**, 110972 (2020).

32) Sanghavi, M. & Rutherford, J. D. Cardiovascular physiology of pregnancy. *Circulation* **130**, 1003–1008 (2014).

33) Mihl, C., Dassen, W. R. M. & Kuipers, H. Cardiac remodelling: concentric versus eccentric hypertrophy in strength and endurance athletes. *NHJL* **16**, 129–133 (2008).

34) Dorn, G. W. The fuzzy logic of physiological cardiac hypertrophy. *Hypertension* **49**, 962–970 (2007).

35) Saheera, S. & Krishnamurthy, P. Cardiovascular Changes Associated with Hypertensive Heart Disease and Aging. *Cell Transplant* **29**, 0963689720920830 (2020).

36) Li, L. *et al.* The role of autophagy in cardiac hypertrophy. *ABBS* **48**, 491–500 (2016).

37) Tahrir, F. G., Langford, D., Amini, S., Mohseni Ahooyi, T. & Kamel, K. Mitochondrial Quality Control in Cardiac Cells: Mechanisms and Role in Cardiac Cell Injury and Disease. *J Cell Physiol* **234**, 8122–8133 (2019).

38) Fischer, T. H. *et al.* Ca2+/calmodulin-dependent protein kinase II equally induces sarcoplasmic reticulum Ca2+ leak in human ischaemic and dilated cardiomyopathy. *European Journal of Heart Failure* **16**, 1292–1300 (2014).

39) Ling, H. *et al.* Requirement for Ca^{2+}/calmodulin–dependent kinase II in the transition from pressure overload–induced cardiac hypertrophy to heart failure in mice. *J Clin Invest* **119**, 1230–1240 (2009).

40) Sciarretta, S., Volpe, M. & Sadoshima, J. Mammalian Target of Rapamycin Signaling in Cardiac Physiology and Disease. *Circulation Research* **114**, 549–564 (2014).

41) Sciarretta, S., Forte, M., Frati, G. & Sadoshima, J. New Insights Into the Role of mTOR Signaling in the Cardiovascular System. *Circulation Research* **122**, 489–505 (2018).

42) Sciarretta, S., Forte, M., Frati, G. & Sadoshima, J. The complex network of mTOR signalling in the heart. *Cardiovasc Res* **118**, 424–439 (2022).

43) Dirkx, E., da Costa Martins, P. A. & De Windt, L. J. Regulation of fetal gene expression in heart failure. *Biochimica et Biophysica Acta (BBA) - Molecular Basis of Disease* **1832**, 2414–2424 (2013).

44) Horio, T. *et al.* Inhibitory Regulation of Hypertrophy by Endogenous Atrial Natriuretic Peptide in Cultured Cardiac Myocytes. *Hypertension* **35**, 19–24 (2000).

45) Belluardo, P. *et al.* Lack of activation of molecular forms of the BNP system in human grade 1 hypertension and relationship to cardiac hypertrophy. *American Journal of Physiology-Heart and Circulatory Physiology* **291**, H1529–H1535 (2006).

46) Booz, G. W. Putting the Brakes on Cardiac Hypertrophy. *Hypertension* **45**, 341–346 (2005).

47) Holtwick, R. *et al.* Pressure-independent cardiac hypertrophy in mice with cardiomyocyte-restricted inactivation of the atrial natriuretic peptide receptor guanylyl cyclase-A. *J Clin Invest* **111**, 1399–1407 (2003).

48) Wilkins, B. J. & Molkentin, J. D. Calcium–calcineurin signaling in the regulation of cardiac hypertrophy. *Biochemical and Biophysical Research Communications* **322**, 1178–1191 (2004).

49) Molkentin, J. D. *et al.* A Calcineurin-Dependent Transcriptional Pathway for Cardiac Hypertrophy. *Cell* **93**, 215–228 (1998).

50) Wang, Y. Mitogen-activated protein kinases in heart development and diseases. *Circulation* **116**, 1413–1423 (2007).

51) Kehat, I. & Molkentin, J. D. Extracellular Signal-Regulated Kinases 1/2 (ERK1/2) Signaling In Cardiac Hypertrophy. *Ann N Y Acad Sci* **1188**, 96–102 (2010).

52) Bueno, O. F. & Molkentin, J. D. Involvement of Extracellular Signal-Regulated Kinases 1/2 in Cardiac Hypertrophy and Cell Death. *Circulation Research* **91**, 776–781 (2002).

53) Rose, B. A., Force, T. & Wang, Y. Mitogen-Activated Protein Kinase Signaling in the Heart: Angels Versus Demons in a Heart-Breaking Tale. *Physiol Rev* **90**, 10.1152/physrev.00054.2009 (2010).

54) Liang, Q. *et al.* c-Jun N-terminal kinases (JNK) antagonize cardiac growth through cross-talk with calcineurin–NFAT signaling. *EMBO J* **22**, 5079–5089 (2003).

55) Wang, Y. *et al.* Cardiac Muscle Cell Hypertrophy and Apoptosis Induced by Distinct Members of the p38 Mitogen-activated Protein Kinase Family*. *Journal of Biological Chemistry* **273**, 2161–2168 (1998).

56) Zechner, D., Thuerauf, D. J., Hanford, D. S., McDonough, P. M. & Glembotski, C. C. A Role for the p38 Mitogen-activated Protein Kinase Pathway in Myocardial Cell Growth, Sarcomeric Organization, and Cardiac-specific Gene Expression. *Journal of Cell Biology* **139**, 115–127 (1997).

57) Tenhunen, O. *et al.* Mitogen-activated Protein Kinases p38 and ERK 1/2 Mediate the Wall Stress-induced Activation of GATA-4 Binding in Adult Heart*. *Journal of Biological Chemistry* **279**, 24852–24860 (2004).

58) Kim, J. *et al.* Insulin-Like Growth Factor I Receptor Signaling Is Required for Exercise-Induced Cardiac Hypertrophy. *Molecular Endocrinology* **22**, 2531–2543 (2008).

59) Soñanez-Organis, J. G. *et al.* HIF-1α and PPARγ during physiological cardiac hypertrophy induced by pregnancy: Transcriptional activities and effects on target genes. *Gene* **591**, 376–381 (2016).

60) McMullen, J. R. *et al.* Phosphoinositide 3-kinase(p110α) plays a critical role for the induction of physiological, but not pathological, cardiac hypertrophy. *Proceedings of the National Academy of Sciences* **100**, 12355–12360 (2003).

61) Bass-Stringer, S., Tai, C. M. K. & McMullen, J. R. IGF1–PI3K-induced physiological cardiac hypertrophy: Implications for new heart failure therapies, biomarkers, and predicting cardiotoxicity. *Journal of Sport and Health Science* **10**, 637–647 (2021).

62) Gray, G. A. & Gray, N. K. A tail of translational regulation. *eLife* **6**, e29104 (2017).

63) Russell, B., Curtis, M. W., Koshman, Y. E. & Samarel, A. M. Mechanical stress-induced sarcomere assembly for cardiac muscle growth in length and width. *Journal of Molecular and Cellular Cardiology* **48**, 817–823 (2010).

64) Grimes, K. M., Prasad, V. & McNamara, J. W. Supporting the heart: Functions of the cardiomyocyte's non-sarcomeric cytoskeleton. *Journal of Molecular and Cellular Cardiology* **131**, 187–196 (2019).

65) Iemitsu, M. *et al.* Physiological and pathological cardiac hypertrophy induce different molecular phenotypes in the rat. *Am J Physiol Regul Integr Comp Physiol* **281**, R2029-2036 (2001).

66) Yin, Z., Ren, J. & Guo, W. Sarcomeric protein isoform transitions in cardiac muscle: A journey to heart failure. *Biochimica et Biophysica Acta (BBA) - Molecular Basis of Disease* **1852**, 47–52 (2015).

67) Wu, C. Focal Adhesion. *Cell Adh Migr* **1**, 13–18 (2007).

68) Ingber, D. Integrins as mechanochemical transducers. *Current Opinion in Cell Biology* **3**, 841–848 (1991).

69) Dorn, G. W. & Force, T. Protein kinase cascades in the regulation of cardiac hypertrophy. *J Clin Invest* **115**, 527–537 (2005).

70) Steinberg, S. F. & Sussman, M. A. Cardiac Hypertrophy Served With Protein Kinase Cε. *Circulation Research* **96**, 711–713 (2005).

71) Iwata, M. *et al.* PKCε–PKD1 signaling complex at Z-discs plays a pivotal role in the cardiac hypertrophy induced by G-protein coupling receptor agonists. *Biochemical and Biophysical Research Communications* **327**, 1105–1113 (2005).

72) van der Velden, J. & Stienen, G. J. M. Cardiac Disorders and Pathophysiology of Sarcomeric Proteins. *Physiological Reviews* **99**, 381–426 (2019).

73) Strait, J. B. *et al.* Role of protein kinase C-ε in hypertrophy of cultured neonatal rat ventricular myocytes. *American Journal of Physiology-Heart and Circulatory Physiology* **280**, H756–H766 (2001).

74) Nicol, R. L. *et al.* Activated MEK5 induces serial assembly of sarcomeres and eccentric cardiac hypertrophy. *The EMBO Journal* **20**, 2757–2767 (2001).

75) Caporizzo, M. A., Chen, C. Y. & Prosser, B. L. Cardiac microtubules in health and heart disease. *Exp Biol Med (Maywood)* **244**, 1255–1272 (2019).

76) Caporizzo, M. A. & Prosser, B. L. The microtubule cytoskeleton in cardiac mechanics and heart failure. *Nat Rev Cardiol* **19**, 364–378 (2022).

77) ter Keurs, H. E. D. J. Microtubules in Cardiac Hypertrophy. *Circulation Research* **82**, 828–831 (1998).

78) Ng, D. C. H. *et al.* Centrosome Reduction Promotes Terminal Differentiation of Human Cardiomyocytes. *Stem Cell Reports* **15**, 817–826 (2020).

79) Oddoux, S. *et al.* Microtubules that form the stationary lattice of muscle fibers are dynamic and nucleated at Golgi elements. *Journal of Cell Biology* **203**, 205–213 (2013).

80) Fassett, J. T. *et al.* Adenosine regulation of microtubule dynamics in cardiac hypertrophy. *American Journal of Physiology-Heart and Circulatory Physiology* **297**, H523–H532 (2009).

81) Palazzo, A. F., Cook, T. A., Alberts, A. S. & Gundersen, G. G. mDia mediates Rho-regulated formation and orientation of stable microtubules. *Nat Cell Biol* **3**, 723–729 (2001).

82) Siegrist, S. E. & Doe, C. Q. Microtubule-induced cortical cell polarity. *Genes Dev.* **21**, 483–496 (2007).

83) Prins, K. W. *et al.* Colchicine Depolymerizes Microtubules, Increases Junctophilin-2, and Improves Right Ventricular Function in Experimental Pulmonary Arterial Hypertension. *Journal of the American Heart Association* **6**, e006195.

84) Bailey, B. A., Dipla, K., Li, S. & Houser, S. R. Cellular Basis of Contractile Derangements of Hypertrophied Feline Ventricular Myocytes. *Journal of Molecular and Cellular Cardiology* **29**, 1823–1835 (1997).

85) Caporizzo, M. A., Chen, C. Y., Bedi, K., Margulies, K. B. & Prosser, B. L. Microtubules Increase Diastolic Stiffness in Failing Human Cardiomyocytes and Myocardium. *Circulation* **141**, 902–915 (2020).

86) Harris, T. S. *et al.* Constitutive properties of hypertrophied myocardium: cellular contribution to changes in myocardial stiffness. *American Journal of Physiology-Heart and Circulatory Physiology* **282**, H2173–H2182 (2002).

87) Zile, M. R. *et al.* Role of microtubules in the contractile dysfunction of hypertrophied myocardium. *Journal of the American College of Cardiology* **33**, 250–260 (1999).

88) Chen, C. Y. *et al.* Suppression of detyrosinated microtubules improves cardiomyocyte function in human heart failure. *Nat Med* **24**, 1225–1233 (2018).

89) Caporizzo, M. A., Chen, C. Y., Salomon, A. K., Margulies, K. B. & Prosser, B. L. Microtubules Provide a Viscoelastic Resistance to Myocyte Motion. *Biophysical Journal* **115**, 1796–1807 (2018).

90) Yan, K., Wang, K. & Li, P. The role of post-translational modifications in cardiac hypertrophy. *Journal of Cellular and Molecular Medicine* **23**, 3795–3807 (2019).

91) Robison, P. *et al.* Detyrosinated microtubules buckle and bear load in contracting cardiomyocytes. *Science* **352**, aaf0659 (2016).

92) Chinnakkannu, P. *et al.* Site-specific Microtubule-associated Protein 4 Dephosphorylation Causes Microtubule Network Densification in Pressure Overload Cardiac Hypertrophy*. *Journal of Biological Chemistry* **285**, 21837–21848 (2010).

93) Howes, S. C., Alushin, G. M., Shida, T., Nachury, M. V. & Nogales, E. Effects of tubulin acetylation and tubulin acetyltransferase binding on microtubule structure. *Mol Biol Cell* **25**, 257–266 (2014).

94) Xu, Z. *et al.* Microtubules acquire resistance from mechanical breakage through intralumenal acetylation. *Science* **356**, 328–332 (2017).

95) Johnson, V., Ayaz, P., Huddleston, P. & Rice, L. M. Design, Overexpression, and Purification of Polymerization-Blocked Yeast αβ-Tubulin Mutants. *Biochemistry* **50**, 8636–8644 (2011).

96) Ti, S.-C., Wieczorek, M. & Kapoor, T. M. Purification of Affinity Tag-free Recombinant Tubulin from Insect Cells. *STAR Protocols* **1**, 100011 (2020).

97) Vemu, A., Garnham, C. P., Lee, D.-Y. & Roll-Mecak, A. Chapter Nine - Generation of Differentially Modified Microtubules Using In Vitro Enzymatic Approaches. in *Methods in Enzymology* (ed. Vale, R. D.) vol. 540 149–166 (Academic Press, 2014).

98) Li, L., Zhang, Q., Lei, X., Huang, Y. & Hu, J. MAP4 as a New Candidate in Cardiovascular Disease. *Frontiers in Physiology* **11**, (2020).

99) Takahashi, M. *et al.* Phenotypic consequences of β1-tubulin expression and MAP4 decoration of microtubules in adult cardiocytes. *American Journal of Physiology-Heart and Circulatory Physiology* **285**, H2072–H2083 (2003).

100) Cheng, G. *et al.* Basis for MAP4 Dephosphorylation-related Microtubule Network Densification in Pressure Overload Cardiac Hypertrophy*. *Journal of Biological Chemistry* **285**, 38125–38140 (2010).

101) Feng, Y. *et al.* Microtubule associated protein 4 (MAP4) phosphorylation reduces cardiac microvascular density through NLRP3-related pyroptosis. *Cell Death Discov.* **7**, 1–12 (2021).

102) Scholz, D. *et al.* Microtubule-associated protein-4 (MAP-4) inhibits microtubule-dependent distribution of mRNA in isolated neonatal cardiocytes. *Cardiovascular Research* **71**, 506–516 (2006).

103) Li, L. *et al.* Microtubule associated protein 4 phosphorylation leads to pathological cardiac remodeling in mice. *EBioMedicine* **37**, 221–235 (2018).

104) Scarborough, E. A. *et al.* Microtubules orchestrate local translation to enable cardiac growth. *Nat Commun* **12**, 1547 (2021).

105) Kislauskis, E. H., Zhu, X. & Singer, R. H. β-Actin Messenger RNA Localization and Protein Synthesis Augment Cell Motility. *Journal of Cell Biology* **136**, 1263–1270 (1997).

106) Anderson, M. E., Brown, J. H. & Bers, D. M. CaMKII in myocardial hypertrophy and heart failure. *Journal of Molecular and Cellular Cardiology* **51**, 468–473 (2011).

107) Tanaka, S., Fujio, Y. & Nakayama, H. Caveolae-Specific CaMKII Signaling in the Regulation of Voltage-Dependent Calcium Channel and Cardiac Hypertrophy. *Frontiers in Physiology* **9**, (2018).

108) Backs, J. *et al.* The δ isoform of CaM kinase II is required for pathological cardiac hypertrophy and remodeling after pressure overload. *Proceedings of the National Academy of Sciences* **106**, 2342–2347 (2009).

109) Zhang, T. *et al.* The Cardiac-specific Nuclear δB Isoform of Ca2+/Calmodulin-dependent Protein Kinase II Induces Hypertrophy and Dilated Cardiomyopathy Associated with Increased Protein Phosphatase 2A Activity*. *Journal of Biological Chemistry* **277**, 1261–1267 (2002).

110) Yu, X. *et al.* MARK4 controls ischaemic heart failure through microtubule detyrosination. *Nature* **594**, 560–565 (2021).

111) Böhm, H., Brinkmann, V., Drab, M., Henske, A. & Kurzchalia, T. V. Mammalian homologues of C. elegans PAR-1 are asymmetrically localized in epithelial cells and may influence their polarity. *Current Biology* **7**, 603–606 (1997).

112) Suzuki, A. & Ohno, S. The PAR-aPKC system: lessons in polarity. *Journal of Cell Science* **119**, 979–987 (2006).

113) Wu, Y. & Griffin, E. E. Chapter Eleven - Regulation of Cell Polarity by PAR-1/MARK Kinase. in *Current Topics in Developmental Biology* (ed. Jenny, A.) vol. 123 365–397 (Academic Press, 2017).

114) Cohen, D., Fernandez, D., Lázaro-Diéguez, F. & Müsch, A. The serine/threonine kinase Par1b regulates epithelial lumen polarity via IRSp53-mediated cell-ECM signaling. *J Cell Biol* **192**, 525–540 (2011).

115) Goldstein, B. & Macara, I. G. The PAR Proteins: Fundamental Players in Animal Cell Polarization. *Developmental Cell* **13**, 609–622 (2007).

116) Gu, G. J. *et al.* Elevated MARK2-Dependent Phosphorylation of Tau in Alzheimer's Disease. *Journal of Alzheimer's Disease* **33**, 699–713 (2013).

117) Sapir, T. *et al.* Accurate Balance of the Polarity Kinase MARK2/Par-1 Is Required for Proper Cortical Neuronal Migration. *J. Neurosci.* **28**, 5710–5720 (2008).

118) Tublin, J. M., Adelstein, J. M., del Monte, F., Combs, C. K. & Wold, L. E. Getting to the Heart of Alzheimer Disease. *Circulation Research* **124**, 142–149 (2019).

119) Snyder, H. M. *et al.* Vascular contributions to cognitive impairment and dementia including Alzheimer's disease. *Alzheimer's & Dementia* **11**, 710–717 (2015).

120) Yamahashi, Y., Saito, Y., Murata-Kamiya, N. & Hatakeyama, M. Polarity-regulating Kinase Partitioning-defective 1b (PAR1b) Phosphorylates Guanine Nucleotide

Exchange Factor H1 (GEF-H1) to Regulate RhoA-dependent Actin Cytoskeletal Reorganization*. *Journal of Biological Chemistry* **286**, 44576–44584 (2011).

121) Ponnusamy, L., Natarajan, S. R. & Manoharan, R. MARK2 potentiate aerobic glycolysis-mediated cell growth in breast cancer through regulating mTOR/HIF-1α and p53 pathways. *Journal of Cellular Biochemistry* **123**, 759–771 (2022).

122) Zeng, Y. *et al.* MARK2 regulates chemotherapeutic responses through class IIa HDAC-YAP axis in pancreatic cancer. *Oncogene* **41**, 3859–3875 (2022).

123) Wang, Y.-C., Khan, Z., Kaschube, M. & Wieschaus, E. F. Differential positioning of adherens junctions is associated with initiation of epithelial folding. *Nature* **484**, 390–393 (2012).

124) Suzuki, A. *et al.* aPKC Acts Upstream of PAR-1b in Both the Establishment and Maintenance of Mammalian Epithelial Polarity. *Current Biology* **14**, 1425–1435 (2004).

125) Dai, Y., Luo, W. & Chang, J. Rho kinase signaling and cardiac physiology. *Current Opinion in Physiology* **1**, 14–20 (2018).

126) Lauriol, J. *et al.* RhoA signaling in cardiomyocytes protects against stress-induced heart failure but facilitates cardiac fibrosis. *Science Signaling* **7**, ra100–ra100 (2014).

127) Lin, J., Hou, K. K., Piwnica-Worms, H. & Shaw, A. S. The Polarity Protein Par1b/EMK/MARK2 Regulates T Cell Receptor-Induced Microtubule-Organizing Center Polarization1. *The Journal of Immunology* **183**, 1215–1221 (2009).

128) Wu, G., Ge, J., Huang, X., Hua, Y. & Mu, D. Planar Cell Polarity Signaling Pathway in Congenital Heart Diseases. *BioMed Research International* **2011**, e589414 (2011).

129) Henderson, D. J., Phillips, H. M. & Chaudhry, B. Vang-like 2 and Noncanonical Wnt Signaling In Outflow Tract Development. *Trends in Cardiovascular Medicine* **16**, 38–45 (2006).

130) Rohr, S., Bit-Avragim, N. & Abdelilah-Seyfried, S. Heart and soul/PRKCi and nagie oko/Mpp5 regulate myocardial coherence and remodeling during cardiac morphogenesis. *Development* **133**, 107–115 (2006).

131) Phillips, H. M. *et al.* Disruption of Planar Cell Polarity Signaling Results in Congenital Heart Defects and Cardiomyopathy Attributable to Early Cardiomyocyte Disorganization. *Circulation Research* **101**, 137–145 (2007).

132) Higashi, M. *et al.* Long-Term Inhibition of Rho-Kinase Suppresses Angiotensin II–Induced Cardiovascular Hypertrophy in Rats In Vivo. *Circulation Research* **93**, 767–775 (2003).

133) Kluge, A. *et al.* Original article - Rho-family GTPase 1 (Rnd1) is a biomechanical stress-sensitive activator of cardiomyocyte hypertrophy. *Journal of Molecular and Cellular Cardiology* **129**, 130–143 (2019).

134) Noma, K., Oyama, N. & Liao, J. K. Physiological role of ROCKs in the cardiovascular system. *American Journal of Physiology-Cell Physiology* **290**, C661–C668 (2006).

135) Guo, S. & Kemphues, K. J. par-1, a gene required for establishing polarity in C. elegans embryos, encodes a putative Ser/Thr kinase that is asymmetrically distributed. Cell 81, 611–620 (1995).

136) Matenia, D. & Mandelkow, E.-M. The tau of MARK: a polarized view of the cytoskeleton. *Trends in Biochemical Sciences* **34**, 332–342 (2009).

137) Abdul-Ghani, M. *et al.* Cardiotrophin 1 stimulates beneficial myogenic and vascular remodeling of the heart. *Cell Res* **27**, 1195–1215 (2017).

138) Timm, T. *et al.* Microtubule Affinity Regulating Kinase Activity in Living Neurons Was Examined by a Genetically Encoded Fluorescence Resonance Energy Transfer/Fluorescence Lifetime Imaging-based Biosensor: INHIBITORS WITH THERAPEUTIC POTENTIAL*. *Journal of Biological Chemistry* **286**, 41711–41722 (2011).

139) Zile, M. R. *et al.* Cardiocyte cytoskeleton in patients with left ventricular pressure overload hypertrophy. *Journal of the American College of Cardiology* **37**, 1080–1084 (2001).

140) Engel, F. B., Schebesta, M. & Keating, M. T. Anillin localization defect in cardiomyocyte binucleation. *Journal of Molecular and Cellular Cardiology* **41**, 601–612 (2006).

141) Bishop, S. P., Zhou, Y., Nakada, Y. & Zhang, J. Changes in Cardiomyocyte Cell Cycle and Hypertrophic Growth During Fetal to Adult in Mammals. *Journal of the American Heart Association* **10**, e017839 (2021).

142) Vliegen, H. W., Eulderink, F., Bruschke, A. V., van der Laarse, A. & Cornelisse, C. J. Polyploidy of myocyte nuclei in pressure overloaded human hearts: a flow cytometric study in left and right ventricular myocardium. *Am J Cardiovasc Pathol* **5**, 27–31 (1995).

143) Adler, C. P. & Friedburg, H. Myocardial DNA content, ploidy level and cell number in geriatric hearts: Post-mortem examinations of human myocardium in old age. *Journal of Molecular and Cellular Cardiology* **18**, 39–53 (1986).

144) Belmadani, S., Poüs, C., Fischmeister, R. & Méry, P.-F. Post-translational modifications of tubulin and microtubule stability in adult rat ventricular myocytes and immortalized HL-1 cardiomyocytes. *Mol Cell Biochem* **258**, 35–48 (2004).

145) Pasapera, A. M. *et al.* MARK2 regulates directed cell migration through modulation of myosin II contractility and focal adhesion organization. *Current Biology* **32**, 2704-2718.e6 (2022).

146) Cohen, D., Brennwald, P. J., Rodriguez-Boulan, E. & Müsch, A. Mammalian PAR-1 determines epithelial lumen polarity by organizing the microtubule cytoskeleton. *Journal of Cell Biology* **164**, 717–727 (2004).

147) Trinczek, B., Brajenovic, M., Ebneth, A. & Drewes, G. MARK4 Is a Novel Microtubule-associated Proteins/Microtubule Affinity-regulating Kinase That Binds to the Cellular Microtubule Network and to Centrosomes*. *Journal of Biological Chemistry* **279**, 5915–5923 (2004).

148) Fassett, J. T. *et al.* Microtubule Actin Cross-Linking Factor 1 Regulates Cardiomyocyte Microtubule Distribution and Adaptation to Hemodynamic Overload. *PLOS ONE* **8**, e73887 (2013).

149) Cooper, G. Cytoskeletal networks and the regulation of cardiac contractility: microtubules, hypertrophy, and cardiac dysfunction. *American Journal of Physiology-Heart and Circulatory Physiology* **291**, H1003–H1014 (2006).

150) Tsutsui, H. *et al.* Role of microtubules in contractile dysfunction of hypertrophied cardiocytes. *Circulation* **90**, 533–555 (1994).

151) Dumont, N. A. & Rudnicki, M. A. Targeting muscle stem cell intrinsic defects to treat Duchenne muscular dystrophy. *npj Regen Med* **1**, 1–7 (2016).

152) Zhang, S. *et al.* In-Cell NMR Study of Tau and MARK2 Phosphorylated Tau. *Int J Mol Sci* **20**, 90 (2018).

153) Ando, K. *et al.* Tau phosphorylation at Alzheimer's disease-related Ser356 contributes to tau stabilization when PAR-1/MARK activity is elevated. *Biochemical and Biophysical Research Communications* **478**, 929–934 (2016).

154) Maina, M. B. *et al.* The involvement of tau in nucleolar transcription and the stress response. *acta neuropathol commun* **6**, 1–13 (2018).

155) Rossi, G. *et al.* Mutations in MAPT Gene Cause Chromosome Instability and Introduce Copy Number Variations Widely in the Genome. *Journal of Alzheimer's Disease* **33**, 969–982 (2013).

156) Frost, B., Hemberg, M., Lewis, J. & Feany, M. B. Tau promotes neurodegeneration through global chromatin relaxation. *Nat Neurosci* **17**, 357–366 (2014).

157) Guo, C. *et al.* Tau Activates Transposable Elements in Alzheimer's Disease. *Cell Reports* **23**, 2874–2880 (2018).

158) Zebrowski, D. C. *et al.* Developmental alterations in centrosome integrity contribute to the post-mitotic state of mammalian cardiomyocytes. *eLife* **4**, e05563 (2015).

159) Leone, M., Musa, G. & Engel, F. B. Cardiomyocyte binucleation is associated with aberrant mitotic microtubule distribution, mislocalization of RhoA and IQGAP3, as well as defective actomyosin ring anchorage and cleavage furrow ingression. *Cardiovascular Research* **114**, 1115–1131 (2018).

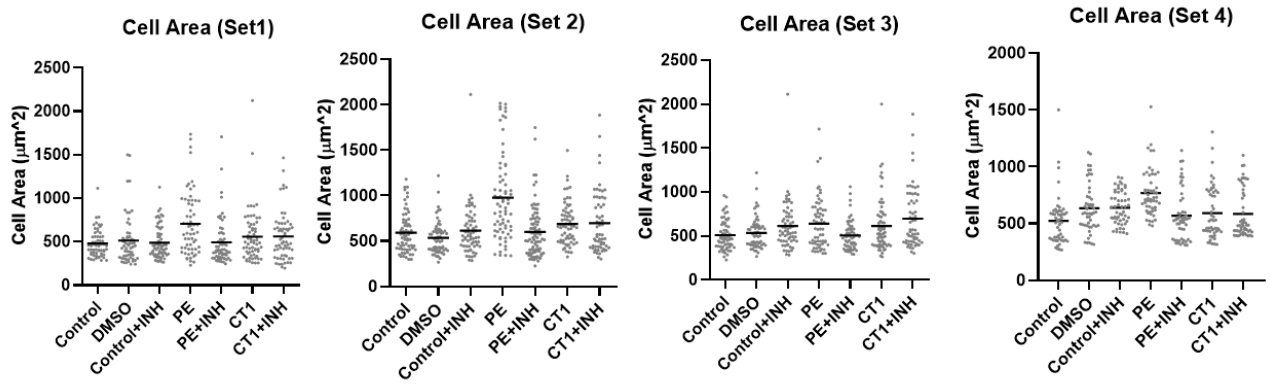

Appendix Figure 1 MARK2 affects the morphological structure of cardiomyocytes in pathological hypertrophy (expanded individual sets). Primary neonatal cardiomyocytes stimulated were either pretreated with MARK2 kinase activity inhibitor 39621 (20µM; DMSO) followed by either 24 h with phenylephrine (PE), α-adrenergic agonist (100 µM), and human cardiotrophin 1 (hCT1) (0.5 nM), or control serum-free medium (Ctrl) followed by morphometric analysis. Quantification of the average cell surface area(A) determined via imageJ and all data are expressed as mean ± SEM. 60 cells per group were used for analysis.